Energy Dissipation In Vibrating Structures

A First Year Report
Submitted to the University of Cambridge

By
Sondipon Adhikari

Trinity College

Cambridge University Engineering Department

May 14, 1998

Preface

Characterisation of damping forces in vibrating structures has always been an active area of research in structural dynamics. Although the topic of damping is an old problem, it has gained momentum in the recent years due to modern engineering developments such as composite materials and structural control. In-spite of a large amount of research, knowledge of damping mechanisms and generic methodologies for handling them in the equations of motion have not been developed yet. The present report is aimed at contributing new methodologies in achieving solution of damped equations of motion, and developing procedures for identification of damping in the context of general vibrating structures. The analysis is limited to linear structural behaviour. The report is divided into three chapters and is appended with a list of references.

A review of the literature on damping within the scope of modal analysis is presented in Chapter 1. Different models of damping used in the context of linear structural vibrations and currently available analysis methods for non-classically damped structures and experimental determination of damping parameters have been reviewed. Limitations of the presently available techniques for dynamic analysis of damped structures and some of the open questions requiring further research are brought out. The motivation for focusing attention on use of complex modes is highlighted.

In Chapter 2, the conventional modal analysis method for linear continuous system is extended to handle general locally reacting damping models. On the account of non-proportional nature of the damping the natural frequencies and mode shapes become complex. Based on the small damping assumption, simple expressions of the natural frequencies and mode shapes have been obtained in terms of undamped system natural frequencies and mode shapes. In conjunction with the above formulation, a method has been proposed to detect the spatial distribution of damping in vibrating structures. The approach is fairly straight-

forward and easily amenable to the conventional modal testing procedures. Information of the complex modes and natural frequencies appears to be sufficient to carry out the proposed method. Validity of the suggested procedure is verified by applying it to two commonly occurred problems in structural dynamics: an axially vibrating rod and an N spring-mass oscillator. For most of the test cases considered the developed method predicts the location of the damping with a sufficient accuracy.

Finally, in Chapter 3 a *research proposal* has been sketched which hopefully will lead us towards a better understanding of the models of damping and its effect on the vibrational response of engineering structures.

Acknowledgements

I am very grateful to my supervisor Dr Jim Woodhouse for his technical guidance and encouraging association throughout the first year of my research work in Cambridge. I would also like to thank Prof Langley for his interest into my research.

I would like to express my gratitude to *Nehru Memorial Trust*, London, *Cambridge Commonwealth Trust* and *Trinity College*, Cambridge for providing the financial support of my research.

I am also thankful to my colleagues in the Mechanics Group of the Cambridge University Engineering Department for providing a congenial atmosphere in the lab without which this work might not come into this shape. Finally, I want to thank my parents for their constant mental support and inspiration, in spite of being far away from me.

Contents

List of Figures

List of Tables

Nomenclature

Chapter 2

$\mathbf{r}$: spatial position vector

t: time

$U(\mathbf{r}, t)$: time-varying displacement function

$\rho(\mathbf{r})$: mass density

L_1: damping operator

L_2: stiffness operator

$p(\mathbf{r}, t)$: distributed time-varying forcing function

M_1, M_2: operators for the boundary conditions

$C_1(\mathbf{r}, \xi, t)$: general kernel function

$\delta(.)$: Dirac delta function

$F(t)$: rate of energy dissipation

$C(\mathbf{r})$: spatial viscous damping function

$g(\mathbf{r}, \tau)$: general locally reacting damping function

$\phi_k(\mathbf{r})$, $k = 1, 2 \cdots \infty$: undamped mode shapes for a system with dissipation function

ω: frequency

ω_k, $k = 1, 2 \cdots \infty$: undamped system natural frequencies

δ_{jk}: Kroneker's delta function

α_k, $k = 1, 2 \cdots \infty$: complex constants

C'_{kj}: elements of modal damping matrix for a dissipation function model

i: unit complex number, $\sqrt{-1}$

$\bar{\phi}_k(\mathbf{r})$, $k = 1, 2 \cdots \infty$: complex mode shapes of system with dissipation function

$\bar{\omega}_k(\mathbf{r})$, $k = 1, 2 \cdots \infty$: complex system natural frequencies

$H(\mathbf{r}, \mathbf{z}, \omega)$: transfer function between the points $\mathbf{r}$ and $\mathbf{z}$ for the system with dissipation function

$F(\omega)$: rate of energy dissipation in time domain

$U(\mathbf{r},\omega)$: displacement function in the frequency domain
$G(\mathbf{r},\omega)$: Fourier transform of the kernel function $g(\mathbf{r},t)$ $G'_{kj}(\omega)$: elements of modal damping matrix for a general damping function model
$\varphi_k(\mathbf{r})$, $k = 1, 2 \cdots \infty$: undamped mode shapes for a system with general damping
$\bar{\varphi}_k(\mathbf{r})$, $k = 1, 2 \cdots \infty$: complex mode shapes of system with general damping
$\mathcal{H}(\mathbf{r},\mathbf{z},\omega)$: transfer function between the points $\mathbf{r}$ and $\mathbf{z}$ for the system with general damping
L: length of the axially vibrating rod
AE: axial rigidity of the axially vibrating rod
$g_t(t)$: time dependent damping function
A_1, A_2 and A_3: area under the damping functions
t_1, λ, t_3 and g_x: constants for different damping models
$H_{ij}(\omega)$: measured transfer functions
$\Delta\omega_n$: bandwidth parameter for the n-th mode
a_n: amplitude factor for the n-th mode
ξ_n: damping factor for the n-th mode
Q_n: Quality factor for the n-th mode
$u_n(x), u_n(y)$: measured mode shapes
$H'(x,y,\omega)$: reconstructed transfer functions
N: number of degree of freedom
$\mathbf{U}$: real part of the complex modal matrix $\left[\bar{\mathbf{\Phi}}\right]$
$\mathbf{V}$: imaginary part of the complex modal matrix $\left[\bar{\mathbf{\Phi}}\right]$
$c(\mathbf{r},\mathbf{z})$: fitted dissipation function for continuous systems
$\mathbf{c}$: fitted dissipation function matrix for discrete systems

Notations

$|.|$: absolute value
$\| \, . \, \|$: Eucledian norm (L_2) for vectors
$\dot{()}$: derivative with respect to time
$(.)^*$: complex conjugation
$\Re(.)$: real part of $(.)$
$\Im(.)$: imaginary part of $(.)$
$(.)^t$: matrix transpose
$< \, . \, >$: inner product norm of vectors

Abbreviations

SDOF: single degree of freedom
MDOF: multiple degrees of freedom
DOF: degrees of freedom
FEM: finite element method

Chapter 1

A REVIEW OF LITERATURE

1.1 Introduction

Characterisation of damping forces in a vibrating structure has always been an active area of research among the researchers in structural dynamics. Since the publication of Lord Rayleigh's classic monograph (1945, originally in 1897) a large body of literature can be found on damping. Although the topic of damping is an age old problem, it has gained momentum in the recent past due to modern engineering demands. Increasing use of composite structural materials in the industry requires development of new reliable damping models. Studies of damping also have a major role in vibration isolation in automobiles under random loading due to surface irregularities and buildings subjected to earthquake loadings. Besides, the recent developments in the fields of robotics and active structures have provided impetus towards developing procedures for dealing with general dissipative forces in the context of structural dynamics.

In-spite of a large amount of research, knowledge of damping mechanisms and a generic methodology for handling them in the equations of motion have not been developed. A main reason for this is unlike inertia and stiffness forces it is not in general clear what are the *state variables* that affect the damping forces. Moreover, it seems that in a realistic situation it is often the structural joints which are more responsible for the energy dissipation than the (solid) material. There have been detailed studies on the material damping (see Bert, 1973) and also on energy dissipation mechanisms in the joints (Earls, 1966, Beards and Williams, 1977). But here difficulty lies in representing all these tiny mechanisms in different parts of the structure in the global equation of motion. Even in many cases these mechanisms turn out be locally non-linear, requiring an equivalent linearisation technique for a global analysis (Bandstra, 1983). A well known method to get rid of all these problems is to use the so called 'viscous damping'. This model supposes that the instantaneous generalised velocities are the only relevant state variables that affect damping. Rayleigh further made one more assumption on this by taking the viscous damping forces to be proportional to inertia and stiffness forces. Since its introduction, this model have been used extensively and now known as 'Rayleigh damping' or 'classical damping'. In this chapter we begin the literature review by

introducing the concept of classical and non-classical damping. Different models of damping used in the context of linear structural vibration and currently available analysis methods for non-classically damped structures and experimental determination of damping parameters have been reviewed. Some open problems requiring further attention and motivation for the study taken up in this report have been highlighted in the concluding section.

1.2 Classical and Non-Classical damping

The equations of motion of an N-degree-of-freedom linear discretetized system with viscous damping can be expressed as

$$\mathbf{M}\ddot{\mathbf{X}} + \mathbf{C}\dot{\mathbf{X}} + \mathbf{K}\mathbf{X} = \mathbf{P}(t) \tag{1.1}$$

where $\mathbf{M}$, $\mathbf{C}$ and $\mathbf{K}$ are respectively the mass, damping and stiffness matrices, $\mathbf{X}$ is the displacement vector and $\mathbf{P}(t)$ is the forcing vector. This equation is a set of coupled second-order differential equation and can be obtained by using Lagrange's equation of motion for small oscillation around the equilibrium (see Meirovitch, 1967). The solution of (1.1) requires information of the initial conditions in terms of the displacement and velocities at all the coordinates. The main methods of solving this equation are the direct integration method and the mode superposition method. The latter method, commonly known as modal analysis, involves computing the response of each mode separately and then summing up the response of all modes of interest to obtain the overall response. For many problems, this offers greater insight into the system behaviour than the direct integration method. It also proves convenient for formulating the problem of identification of structures from the experimental data in terms of normal modes. The first step towards the modal analysis is to consider the undamped (*i.e.* $\mathbf{C} = 0$ in equation 1.1) equation of motion

$$\mathbf{M}\ddot{\mathbf{X}} + \mathbf{K}\mathbf{X} = \mathbf{P}(t) \tag{1.2}$$

Since $\mathbf{M}$ and $\mathbf{K}$ are symmetric matrices it is always possible to find a transformation

$$\mathbf{X} = \mathbf{U}\mathbf{q} \tag{1.3}$$

such that equation (1.2) can be uncoupled to give

$$\ddot{\mathbf{q}} + \mathbf{\Lambda}\mathbf{q} = \phi(t) \tag{1.4}$$

where $\phi(t) = \mathbf{U}^t\mathbf{P}(t)$ with $(\bullet)^t$ denoting matrix transpose, and $\mathbf{\Lambda}$ is a diagonal matrix whose elements are the natural frequencies squared. In equation (1.3), $\mathbf{U}$ is the $N \times N$ matrix of system displacement eigenvectors or normal modes. Now, for the damped equation of motion (1.1), the transformation to the normal coordinates leads to

$$\ddot{\mathbf{q}} + \mathbf{U}^t\mathbf{C}\mathbf{U} + \mathbf{\Lambda}\mathbf{q} = \phi(t) \tag{1.5}$$

This equation will be uncoupled if and only if $\mathbf{U}^t\mathbf{C}\mathbf{U}$ is diagonal. It is easy to see that there is no definite mathematical reason why $\mathbf{U}^t\mathbf{C}\mathbf{U}$ should always be diagonal and allow modal analysis method to be used. Rayleigh (1897) pointed out that if the $\mathbf{C}$ matrix has the from

$$\mathbf{C} = \alpha\mathbf{M} + \beta\mathbf{K} \tag{1.6}$$

then the damped equations of motion in normal coordinates (1.5) can be decoupled. This damping model is known as 'Rayleigh damping' or 'classical damping'. It is important to note that the notion of classical damping has arisen in the context of simultaneous diagonalisation of the damped equations of motion, and is not based on any physical mechanism of damping. It is well possible that for most of the systems we consider, the mechanism of damping will not follow equation (1.6). Realising this Caughey (1960) has proposed a more general form of damping matrix which will lead to uncoupling of equation of motion and can be given by

$$\mathbf{C} = \alpha\mathbf{M}\sum_{\mathbf{k=0}}^{\mathbf{p-1}} a_k\left[\mathbf{M^{-1}K}\right]^k \tag{1.7}$$

In this case the modal damping matrix is given by (Bathe, 1982)

$$\mathbf{U}^t\mathbf{C}\mathbf{U} = \mathrm{diag}(2\zeta_i\omega_i) = \mathrm{diag}\left[a_0 + a_1\omega_i^2 + a_2\omega_i^4 + \cdots a_{p-1}\omega_i^{2p-3}\right] \tag{1.8}$$

From the above series it is clear that Rayleigh Damping assumption is a special case of this expression with $p = 2$ (*i.e.* the first two term in the series). Caughey and O'Kelly (1965) have given necessary and sufficient conditions under which a damped dynamic system possesses classical normal modes. It has been shown that if $\mathbf{M}^{-1}\mathbf{C}$ commutes with $\mathbf{M}^{-1}\mathbf{K}$ then there exist a real congruence transformation which simultaneously diagonalises $\mathbf{M}$, $\mathbf{C}$ and $\mathbf{K}$. This result was further generalised by Caughey and O'Kelly (1965) as commutativity of stiffness and damping operator in modal coordinates (provided the inertia operator is assumed to be algebraic, whereas the damping and stiffness operator are allowed to be linear differential operators). So if a damped system is to possess real modes, they must coincide with the classical normal modes.

A system is called non-classically damped if it is not possible to simultaneously diagonalise $\mathbf{M}$, $\mathbf{C}$ and $\mathbf{K}$. It is obvious that for any general damping matrix a dynamic system will not have classical normal modes since the series given by equation (1.8) does not form a complete set of functions. In this case the eigenvalues and eigenvectors of the system become complex. Nicholson and Baojiu (1996), Nicholson (1987a) have reviewed the literature on stable response of non-classically damped mechanical systems. It has been pointed out by Nicholson (1987a) that in some of the application areas, for example control in vehicle dynamics, the mass and stiffness matrices no longer remain symmetric. In view of non-symmetric mass and stiffness matrices the notion of non-classical damping introduced earlier also changes since in general it is not possible to find a real transformation which simultaneously diagonalises the mass and stiffness matrices themselves. These kinds of system are

known as non-conservative systems. Several authors like Fawzy and Bishop (1976), Washed and Bishop (1976), Fawzy (1977), and Bishop and Price (1979) have considered the vibration of asymmetric dynamical systems. Inman (1983) has given necessary and sufficient conditions for the existence of a linear transformation that transforms an asymmetric system into an equivalent symmetric system. He has also shown that a certain class of asymmetric damped linear dynamical system can have similar behaviour to an associated symmetric system. Ahmadian and Inman (1984a) have generalised the above results to non-classical symmetrizable system with the use of similarity transformations. Ahmadian and Inman (1984b) have further analysed criticality of damping for non-classical symmetrizable system. Caughey and Ma (1993) have considered the necessary and sufficient conditions for decoupling of a general non-classical discrete linear dynamical system. They have considered a system like (1.1) but in that $\mathbf{M}$, $\mathbf{C}$ and $\mathbf{K}$ are not symmetric positive definite. It has been proved by them that this system can only be decoupled if the coefficient matrices $\mathbf{M}$, $\mathbf{C}$ and $\mathbf{K}$ are diagonalisable and pairwise commutative, *i.e.* $\mathbf{MC} = \mathbf{CM}$, $\mathbf{MK} = \mathbf{KM}$ and $\mathbf{CK} = \mathbf{KC}$. However, in this case the diagonalizing matrix (mode shapes) is in general complex in nature. Ma and Caughey (1995) have extended the classical modal analysis to linear conservative systems by utilising equivalence transformations in Lagrangian coordinates.

From the above discussions we can say that in the context of current literature the notion of non-classical damping becomes subjective. If the mass and stiffness matrix is non-symmetric then the concept of non-proportional damping introduced earlier loses its meaning. However, in the subsequent discussions in this chapter mass and stiffness matrix will be assumed to be symmetric positive definite and non-classically damped system should be viewed with reference to this kind of system only.

1.3 Different Models of Damping

Damping is the dissipation of energy from a vibrating system. In this context, the term dissipate is used to mean the transformation of energy into the other form of energy and, therefore, a removal of energy from the vibrating system. The type of energy into which the mechanical energy is transformed is dependent on the system and the physical mechanism that cause the dissipation. For most vibrating system, a significant part of the energy is converted into heat.

The specific ways in which energy is dissipated in vibration are dependent upon the physical mechanisms active in the structure. These physical mechanisms are complicated physical process that are not totally understood. The types of damping that are present in the structure will depend on what mechanism that are predominant in the given situation. Thus, any mathematical representation of the physical damping mechanisms in the equations of motion of a vibrating system will have to be a generalisation and approximation of the true physical situation. As Scanlan (1970) has observed, any mathematical damping model is really only a crutch which does not give a detailed explanation of the underlying physics.

For our mathematical convenience, we divide the elements that dissipate energy into

two classes: the discrete elements and the continuous elements. Elements such as dampers of a vehicle-suspension fall in the first class. Dissipation within a solid body, on the other hand, falls in the second class, demands a representation which accounts for both its intrinsic properties and its spatial distribution. There have been attempt to mathematically describe the damping in both discrete and continuous systems.

Free oscillation of an undamped SDOF system never die out and the simplest approach to introduce dissipation is to incorporate an ideal viscous dashpot in the model. The damping force is assumed to be proportional to the velocity and the coefficient of proportionality is known as the dashpot-constant. The loss factor, which is the energy dissipation per radian to the peak potential energy in the cycle, is widely accepted as a basic measure of the damping. For a SDOF system this loss factor can be given by

$$\eta = \frac{c|\omega|}{k} \tag{1.9}$$

where c is the viscous damping constant and k is the stiffness. The above equation shows a linear dependence of the loss factor on the driving frequency. This dependence has been discussed by Crandall (1970) where it has been pointed out that the frequency dependence, observed in practice, is usually not of this form. In such cases one often resorts to an equivalent ideal dashpot. Theoretical objections to the approximately constant value of damping over a range of frequency, as observed in aeroelasticity problems, have been raised by Naylor (1970). On the lines of equation (1.9) one is tempted to define the frequency-dependent dashpot as

$$c(\omega) = \frac{k\eta(\omega)}{|\omega|} \tag{1.10}$$

This representation, however has some serious physical limitations. Crandall (1970,1991), Newland (1989) and Scanlan (1970) have pointed out that such a representation violates causality, a principle which asserts that the states of a system at a given point of time can be affected only by the events in the past and not by those of the future.

Now for the SDOF system, the frequency domain description of the equation of motion can be given by

$$\left[-m\omega^2 + \mathrm{i}\omega c(\omega) + k\right] X(\mathrm{i}\omega) = F(\mathrm{i}\omega) \tag{1.11}$$

where $X(\mathrm{i}\omega)$ and $F(\mathrm{i}\omega)$ are the response and excitation respectively, represented in the frequency domain. Note that the dashpot is now allowed to have frequency dependence. Inserting equation (1.10) into (1.11) we obtain

$$\left[-m\omega^2 + k\left\{1 + \mathrm{i}\eta(\omega)\mathrm{sgn}(\omega)\right\}\right] X(\mathrm{i}\omega) = F(\mathrm{i}\omega) \tag{1.12}$$

where sgn represents the sign function. The 'time-domain' representations of equations (1.11) and (1.12) are often taken as

$$m\ddot{x} + c(\omega)\dot{x} + kx = f \tag{1.13}$$

and

$$m\ddot{x} + kx\left\{1 + \mathrm{i}\eta(\omega)\mathrm{sgn}(\omega)\right\} = f \tag{1.14}$$

respectively. It has been pointed out by Crandall (1970) that these are not the correct Fourier inverses of equations (1.11) and (1.12). The reason for is that the inertia, the stiffness and the forcing function are inverted properly, while the damping terms in equations (1.13) and (1.14) are obtained by mixing the frequency-domain and time-domain operations. Crandall (1970) calls (1.13) and (1.14) as the 'non-equations' in time domain. It has been pointed out by Newland (1989) that only certain forms of frequency dependence for $\eta(\omega)$ are allowed in order to to satisfy causality. In Crandall (1970) it was shown that the impulse response function for the ideal hysteretic dashpot (η independent of frequency), is given by

$$h(t) = \frac{1}{\pi k \eta_0}.\frac{1}{t}; \qquad -\infty < t < \infty. \tag{1.15}$$

This response function is clearly non-causal since it states that the system responds before the excitation (or the cause) takes place. Crandall (1970) has further shown that a band-limited hysteretic dashpot is also non-causal. In view of this discussion it can be said that the most of the hysteretic damping model fails to satisfy the casualty condition.

The physical mechanisms of damping, including various types of external friction, fluid viscosity, and internal material friction, have been studied rather extensively in some detail and are complicated physical phenomena. However, a certain simplified mathematical formulation of damping forces and energy dissipation can be associated with a class of physical phenomenon. Columb damping, for example is used to represent dry friction present in sliding surfaces, such as springs and structural joints. For this kind of damping, the force resisting motion is assumed to be proportional to the normal force between the sliding surfaces and independent of the velocity except for the sign. The damping force is thus

$$F_d = \frac{\dot{x}}{|\dot{x}|} F_r = \mathrm{sgn}(\dot{x}) F_r \tag{1.16}$$

where F_r is the frictional force. In the context of finding equivalent viscous damping, Bandstra (1983) have reported several mathematical models of physical damping mechanisms in SDOF systems. For example, velocity squared damping, which is present when a mass vibrates in a fluid or when fluid is forced rapidly through an orifice. The damping force (F_d) in this case is

$$F_d = \mathrm{sgn}(\dot{x}) a \dot{x}^2; \qquad \text{or, more generally } \; F_d = c\dot{x}|\dot{x}|^{n-1} \tag{1.17}$$

where c is the damping proportionality constant. Viscous damping is a special case of this type of damping. If the fluid flow is relatively slow *i.e.* laminar, then by letting $n = 1$ from the above equation one obtains

$$F_d = c\dot{x} \tag{1.18}$$

Another major source of damping in a vibrating structure is the structural joints, see Tan (1997) for a recent review. Here, major part of energy loss takes place through air-pumping. The air-pumping phenomenon is associated with damping when air is entrapped

in pockets in the vicinity of a vibrating surface. In these situations, the entrapped air is 'squeezed out' and 'sucked-in' through any available hole. Dissipation of energy takes place in the process of air flow and columb-friction dominates around the joints. Damping This damping behaviour has been studied by many authors in some practical situations, for example Earls (1966) have obtained the energy dissipation in a lap joint over a cycle under different clamping pressure. Beards *et. al.* (1977) have noted that significant damping can be obtained by suitably choosing the fastening pressure at the interfacial slip in joints.

Energy dissipation within the material is attributed to a variety of mechanisms such as thermoelasticity, grainboundary viscosity, point-defect relaxation etc (see Lazan, 1959, 1968, Bert 1973). This in general called material damping. In an imperfect elastic material, the stress-strain curve forms a closed hysteresis loop rather that a single line upon a cyclic loading. Much effort has been devoted by numerous investigators to develop models of hysteretic restoring forces and techniques to identify such systems. For a recent review on this literature we refer the readers to Chassiakos *et. al.*, (1998). Most of these study is motivated by the observed fact that the energy dissipation from materials is only a weak function of frequency and almost directly proportional to x^n. The exponent on displacement for the energy dissipation of material damping ranges from 2 to 3, for example 2.3 for mild steel (Bandstra,1983). In this context, another large body of literature can be found on composite materials where many researchers have evaluated a materials specific damping capacity (SDC). Baburaj and Matsuzaki (1994) and the references therein give an account of research that has been conducted in this area.

Banks and Inman (1991) have considered four different damping models for a composite beam. These models of damping are:

1. *Viscous air damping:* For this model the damping operator in the Euler-Bernoulli equation for beam vibration becomes

$$L_1 = \gamma I_0 \tag{1.19}$$

where I_0 is the identity operator and γ is the viscous damping constant.

2. *Kelvin-Voigt damping:* For this model the damping operator becomes

$$L_1 = c_d I \frac{\partial^5}{\partial x^4 \partial t} \tag{1.20}$$

where I is the moment of inertia and c_d is the strain-rate dependent damping coefficient.

3. *Time hysteresis damping:* For this model the damping operator is assumed as

$$L_1 = \int_{-\infty}^{t} g(s) u_{xx}(x, t+s) \mathrm{d}s; \qquad \text{where } g(s) = \frac{\alpha}{\sqrt{-s}} \exp(\beta s) \tag{1.21}$$

where α and β are constants.

4. *spatial hysteresis damping:*

$$L_1 = \frac{\partial}{\partial x}\left[\int_0^L h(x,\xi)\{u_{xx}(x,t) - u_{xt}(\xi,t)\}\mathrm{d}\xi\right] \tag{1.22}$$

The kernel function $h(x,\xi)$ is defined as

$$h(x,\xi) = \frac{a}{b\sqrt{\pi}}\exp[-(x-\xi)^2/2b^2]$$

where b is some constant.

It was observed by them that the spatial hysteresis model combined with a viscous air damping model results in the best quantitative agreement with the experimental time histories.

1.4 Modal Analysis of Non-Classically Damped Systems

Consider the equations of motion of a general viscous damped system in physical coordinates (1.1). Due to the non-classical nature of the damping this set of N differential equations are coupled through the $\mathbf{U}^t\mathbf{C}\mathbf{U}$ term and can not be reduced to N second-order uncoupled equation. The methods for solving this kind of equation subjected to initial conditions of the form

$$\mathbf{X}(0) = \mathbf{X_0}; \qquad \text{and} \qquad \dot{\mathbf{X}}(0) = \dot{\mathbf{X}}_\mathbf{0} \tag{1.23}$$

follows mainly two routes, the state space method and approximate methods in 'N-space'. Discussion on these two methods are taken up in the following sections.

1.4.1 The State Space Method

The state space method is based on transforming the N second-order coupled equations into a set of $2N$ first-order coupled equations by augmenting the displacement response vectors with the velocities of the corresponding coordinates (see Newland, 1989). Equation (1.1) can be recast as

$$\dot{\mathbf{z}} = \mathbf{A}\mathbf{z} + \mathbf{F} \tag{1.24}$$

where $\mathbf{A}$ is the system matrix, $\mathbf{F}$ the force vector and $\mathbf{z}$ is the $2N \times 1$ response vector in the state space given by

$$\mathbf{A} = \begin{bmatrix} \mathbf{0} & \mathbf{I_n} \\ -\mathbf{M^{-1}}K & -\mathbf{M^{-1}C} \end{bmatrix}; \quad \mathbf{z} = \begin{Bmatrix} \mathbf{X} \\ \dot{\mathbf{X}} \end{Bmatrix}; \quad \text{and } \mathbf{F} = \begin{Bmatrix} \mathbf{0} \\ \mathbf{M^{-1}P} \end{Bmatrix} \tag{1.25}$$

In the above equation $\mathbf{0}$ is the $N \times N$ null matrix and $\mathbf{I_n}$ is the $N \times N$ identity matrix. The eigenvalue problem associated with the above equation is in term of a asymmetric matrix now. Uncoupling of equations in the state space is again possible and has been considered

by Fawzy and Bishop (1976), Meirovitch (1980), Newland (1989) and Veletsos and Ventura (1986). This analysis was further generalised by Newland (1987) for the case of systems involving singular matrices. In the formulation of equation (1.24) the matrix **A** is no longer symmetric, and so eigenvectors are no longer orthogonal with respect to it. In fact, in this case, instead of an orthogonality relationship, one obtains a biorthogonality relationship, after solving the adjoint eigenvalue problem. The complete procedure for uncoupling the equations now involves solving two eigenvalue problems, each of which is double the size of an eigenvalue problem in the modal space. The details of the relevant algebra can be found in Meirovitch (1980). As an alternate to this procedure, equation (1.24) can directly be integrated numerically using a suitable time-marching scheme. It should be noted that these solution procedures are exact in nature. One disadvantage of such an exact method is that it requires significant numerical effort to determine the eigensolutions. The effort required is evidently intensified by the fact that the eigensolutions of a non-classically damped system are complex. From the analyst's view point another disadvantage is the lack of physical insight afforded by this method which is intrinsically numerical in nature.

Recently, starting from equation (1.24), Woodhouse (1998) has shown that coefficients of the transfer function matrix $\mathbf{H}_{mn}(\omega)$, can be obtained in terms of n-dimensional (complex) mode shapes $\bar{\mathbf{u}}$ of system (1.1), and system property matrices as,

$$\mathbf{H}_{mn}(\omega) = \sum_{k=1}^{N} \mathrm{i}\alpha_k \left\{ -\frac{\bar{\mathbf{u}}_m^k \bar{\mathbf{u}}_n^k}{\omega - \bar{\omega}_k} + \frac{\bar{\mathbf{u}}_m^{k^*} \bar{\mathbf{u}}_{\mathbf{n}}^{k^*}}{\omega + \bar{\omega}_k^*} \right\} \tag{1.26}$$

where

$$\alpha_j = \frac{1}{2\lambda_{\mathbf{j}} \bar{\mathbf{u}}^{\mathbf{j}^t} \mathbf{M} \bar{\mathbf{u}}^{\mathbf{j}} + \bar{\mathbf{u}}^{\mathbf{j}^t} \mathbf{C} \bar{\mathbf{u}}^{\mathbf{j}}}$$

This provides a link between analysis methods in state space and modal space.

1.4.2 Methods in N-space

It has been pointed out that the state-space approach towards the solution of equation of motion in the context of linear structural dynamics is not only computationally expensive but also fails to provide the physical insight which modal analysis in N-space offers. However, it may be remembered that in the area of non-linear dynamics, in contrast with the linear dynamics, the state-space method gives good physical insight. So several authors have studied non-classically damped linear systems in modal coordinates by approximate methods. In this section we briefly review the existing methods for this kind of analysis.

Approximate Decoupling Method

Consider the equations of motion of a general linear damped system in modal coordinates (1.5) subjected to initial conditions of the form

$$\mathbf{q}(0) = \mathbf{U}^t \mathbf{X}(0) \qquad \text{and} \qquad \dot{\mathbf{q}}(0) = \mathbf{U}^t \dot{\mathbf{X}}(0). \tag{1.27}$$

Earlier it has been mentioned that due to non-classical nature of the damping this set of N differential equations are coupled through the $\mathbf{C}' = \mathbf{U}^t\mathbf{C}\mathbf{U}$ term. A usual approach in this case is to ignore the off-diagonal terms in the modal damping matrix $\mathbf{C}'$ which couple the equations of motion. This approach is termed the decoupling approximation. For large-scale systems, the computational effort in adopting the decoupling approximation is an order of magnitude smaller than the methods of complex modes. The solution of the decoupled equation would be close to the exact solution of the coupled equations if the non-classical damping terms are sufficiently small. A preliminary discussion on this topic can be found in Meirovitch (1967). Thomson *et. al.* (1974) have studied the effect of neglecting off-diagonal entries of the modal damping matrix through numerical experiments and have proposed a method for improved accuracy. Warburton and Soni (1977) have suggested a criterion for such a diagonalisation so that the computed response is acceptable. Using the frequency domain approach, Hesselman (1976) proposed a criterion for determining whether the equations of motion might be considered practically decoupled if non-classical damping exists. The criterion suggested by him was to have adequate frequency separation between the natural modes.

Using matrix norms Shahruz and Ma (1988) have tried to find an optimal diagonal matrix $\mathbf{C_d}$ in place of $\mathbf{C}'$. An important conclusion emerging from their study is that if $\mathbf{C}'$ is diagonally dominant, then among all approximating diagonal matrices $\mathbf{C_d}$, the one that minimises the error bound is simply the diagonal matrix obtained by omitting the off-diagonal elements of $\mathbf{C}'$. Using analysis in time domain Shahruz (1990) has rigorously proved that if $\mathbf{C_d}$ is obtained form $\mathbf{C}'$ by neglecting the off-diagonal elements of $\mathbf{C}'$, then for small off-diagonal elements of $\mathbf{C}'$ the error in the solution of the approximately decoupled system will be small.

An iterative approach for solving the coupled equations is developed by Udwadia and Esfandiari (1990) based on updating the forcing term appropriately. Felszeghy (1993) presented a method which searches for another coordinate system in the neighbourhood of the normal coordinate system so that in the new coordinate system removal of coupling terms in the equations of motion produces a minimum bound on the relative error introduced in the approximate solution. Hwang and Ma (1993) have shown that the error due to the decoupling approximation can be decomposed into an infinite series and can be summed exactly in the Laplace domain. They also concluded that by solving a small number of additional coupled equations in an iterative fashion, the accuracy of the approximate solution can be greatly enhanced.

From the above mentioned studies it has been believed that either frequency separation between the normal modes (Hesselman, 1976) or some form of diagonal dominance (Shahruz and Ma, 1988) in the modal damping matrix $\mathbf{C}'$ is sufficient for neglecting modal coupling. In contrast to these widely accepted beliefs, using Laplace transform methods, Park *et. al.* (1994) have shown that within the practical range of engineering applications neither the diagonal dominance of the modal damping matrix nor the frequency separation between

the normal modes would be sufficient for neglecting modal coupling. They have also given examples when the effect of modal coupling may even increase following the previous criterion. In the context of approximate decoupling, Shahruz and Srimatsya (1997) have considered error vectors in modal and physical coordinates, say denoted by $\mathbf{e_N}(\bullet)$ and $\mathbf{e_P}(\bullet)$ respectively. They have shown that based on the norm (denoted here as $\| (\bullet) \|$) of these error vectors three cases may arise:

1. $\| \mathbf{e_N}(\bullet) \|$ is small (respectively, large) and $\| \mathbf{e_P}(\bullet) \|$ is small (respectively, large)
2. $\| \mathbf{e_N}(\bullet) \|$ is large but $\| \mathbf{e_P}(\bullet) \|$ is small
3. $\| \mathbf{e_N}(\bullet) \|$ is small but $\| \mathbf{e_P}(\bullet) \|$ is large

From this study, especially in view of case 3, it is clear that the error norms based on the modal coordinates are not reliable to use in the actual physical coordinates. However, they have given conditions when $\| \mathbf{e_N}(\bullet) \|$ will lead to a reliable estimate of $\| \mathbf{e_P}(\bullet) \|$. For a flexible structure with light damping Gawronski and Sawicki (1997) have shown that neglecting off-diagonal terms of the modal damping matrix in most practical cases imposes negligible errors in the system dynamics. They also concluded that the requirement of diagonal dominance of the damping matrix is not necessary in the case of small damping, which relaxes the criterion earlier given by Shahruz and Ma (1988).

Perturbation Techniques

Cronin (1976) has obtained an approximate solution for a non-classically damped system under harmonic excitation by perturbation techniques. Clough and Mojtahedi (1976) considered several methods of treating generally damped systems, and concluded that proportional damping approximation may give unreliable results for many cases. Similarly Duncan and Taylor (1979) have shown that significant errors can be incurred when dynamic analysis of a non-proportionally damped system is based on a truncated set of modes, as is commonly done modelling continuous systems. Chung and Lee (1986) applied perturbation techniques to obtain the eigensolutions of damped systems with weakly non-classical damping. Cronin (1990) has developed an efficient perturbation-based series method to solve the eigenproblem for dynamic systems having non-proportional damping matrix. To illustrate the general applicability of this method Peres-de-Silva *et. al.* (1995) applied it to determine the eigenvalues and eigenvectors of a damped gyroscopic system. More recently in the context of non-proportionally damped gyroscopic systems Malone *et. al.* (1997) have developed a perturbation method which uses an undamped gyroscopic system as the unperturbed system.

Non-Proportionality Index

Prater and Sing (1986) and Nair and Sing (1986) have developed several indices, for example indices based on modal phase difference, modal polygon areas etc, to determine

quantitatively the extent of non-classical damping in discrete systems. Another index based on driving frequency and elements of the modal damping matrix is given by Bellos and Inman (1990). Tong *et. al.* (1994) have developed an analytical index for quantification of non-proportionality for discrete vibratory systems. It has been shown that the fundamental nature of non-proportionality lies in finer decompositions of the damping matrix. Felszeghy (1994) developed a formulation based on biorthonormal eigenvector for modal analysis of non-classically damped discrete systems. The analytical procedure take advantage of simplification that arises when the modal analysis of the motion separated into a classical and non-classical modal vector expansion. Shahruz (1995) have shown that the analytical index given by Tong *et. al.* (1994) solely based on the damping matrix can lead to erroneous results when the driving frequency lies close to a system natural frequency. They have suggested that a suitable index for non-proportionality should include the damping matrix and natural frequencies as well as the excitation vector.

Response Bounds and Frequency Response

Nicholson (1987b) gave upper bounds for the response of non-classically damped systems under impulsive loads and step loads. Yae and Inman (1987) have obtained bound on the displacement response of non-proportionally damped discrete systems in terms of physical parameters of the system and input. They also have observed that the larger the deviation from proportional damping the less accurate their results become.

Bellos and Inman (1990) gives a procedure for computing the transfer functions of a non-proportionally damped discrete system. Their method was based on Laplace transformation of the equation of motion in modal coordinate. Bhaskar (1995) have analysed the behaviour of errors in calculating frequency response function when off-diagonal terms of modal damping matrix is neglected. It has been shown that the exact response can be expressed by an infinite Taylor series and the approximation of ignoring the off-diagonal terms of modal damping matrix is equivalent to retaining one term of the series.

Complex Modal Analysis

Other that the approximate decoupling methods described earlier, another approach towards the analysis of non-proportionally damped linear systems is to use complex modes. Since the original contribution of Caughy and O'Kelly (1965), many papers have been written on complex modes. Several authors, for example, Mitchell (1990), Imregun and Ewins (1995), Lallement and Inman (1995), have given reviews on this subject. Placidi *et. al.* (1991) used a series expansion of complex eigenvectors into the subspace of real modes, in order to identify normal modes from complex eigensolutions. In the context of modal analysis Liang *et. al.* (1992) have posed and analysed the question of whether the existence of complex modes is an indicator of non-proportional damping and how a mode is influenced by damping. Analysing the errors in the use of modal coordinates, Sestieri and Ibrahim (1994) have concluded that

the complex mode shapes are not necessarily the result of high damping. The complexity of the mode shapes is the result of particular damping distributions in the system and depends upon the proximity of the mode shapes. Liu and Sneckenberger (1994) have developed a complex mode theory for a linear vibrating deficient system based on the assumption that it has a complete set of eigenvectors. Complex mode superposition methods have been used by Oliveto and Santini (1996) in the context of soil structure interaction problems. Balmès (1997) has proposed a method to find normal modes and the associated non-proportional damping matrix from the complex modes. He has also shown that a set of complex modes is complete if it verifies a defined properness condition which is used to find complete approximations of identified complex modes. Recently Garvey and Penny (1998) have given a relationship between real and imaginary parts of complex modes for general systems whose mass, stiffness and damping can be expressed by real symmetric matrices. They also observed that the relationship becomes most simple when all roots are complex and the real part of all the roots have same sign.

Based on a small damping assumption, more recently Woodhouse (1998) has given the expression for complex natural frequencies and mode shapes of a linear discrete system with general damping in terms of the real undamped natural frequencies and mode shapes.

1.5 Identification of Damping Parameters

Several methods are available for identifying the damping parameters for single degree of freedom systems for linear and non-linear damping models (see Nashif *et. al.*, 1985). For linear damping models these methods can broadly be described as:

1. *Methods based on transient response of the system:* This is also known as logarithmic decrement method: if y_i and y_{i+i} are heights of two subsequent peaks then the damping ratio ζ can be obtained as
$$\delta = \log_e \left(\frac{y_i}{y_{i+i}} \right) \approx 2\pi\zeta \tag{1.28}$$
For applicability of this method the decay must be exponential.

2. *Methods based on harmonic response of the system:* These methods are based on calculating the half power points and bandwidth from the frequency response curve. It can be shown that the damping factor ζ can be related to a peak of the normalised frequency response curve by
$$|H|_{\max} \approx \frac{1}{2\zeta} \tag{1.29}$$

3. *Methods based on energy dissipation:* Consider the force-deflection behaviour of a spring-mass-damper (equivalent to a block of material) under sinusoidal loading at some particular frequency. In steady sate, considering conservation of energy, energy

loss per cycle (Δu_{cyc}) can be calculated by equating it with the input power. Here it can be shown that the damping factor ζ can be related as

$$2\zeta = \frac{\Delta u_{\text{cyc}}}{2\pi U_{\max}} \tag{1.30}$$

where $U_{\max}$ is maximum energy of the system.

The above mentioned methods, although developed for single-degree-of-freedom systems can be used for multiple degree of freedom system for a single measure doing, say for example a cantilever beam vibrating in the first mode.

For multiple degree-of-freedom systems several methods exist to find out the modal damping parameters, for details see Ewins (1984). Later in section 2.3 these methods we will be discussed with more details. Here we wish to make a note that all of these methods basically find out the modal damping ratio. Thus an intrinsic assumption in these methods is that of proportional damping. However, there have been attempts to find out damping parameters of non-proportionally damped systems in the context of some specific applications. Banks and Inman (1991) have considered the problem of estimating damping parameters in a non-proportionally damped beam. They have taken four different models of damping: viscous air damping, Kelvin-Voigt damping, time hysteresis damping and spatial hysteresis damping, and used a spline inverse procedure to form a least-square fit to the experimental data. A procedure for obtaining hysteretic damping parameters in free-hanging pipe systems is given by Fang and Lyons (1994). Assuming material damping is the only source of damping they have given a theoretical expression for the loss factor of the n-th mode. Their theory predicts higher modal damping ratios in higher modes. Recently Chassiakos *et. al.*, (1998) proposed an on-line parameter identification technique for a single degree of freedom hysteretic system.

1.6 Open Problems and Conclusion

Based on the review of literature presented so far in this chapter, it can be observed that in spite of extensive research effort, many questions are still to be answered. These questions can broadly be divided in three ways, firstly what damping model has to be used, *i.e.* viscous or non-viscous and if non-viscous then what kind of model it could be, secondly the solution procedures for systems with non-proportional damping and thirdly the evaluation of the damping parameters if a system is non-proportional. The first question is a major issue, and in the context of general analysis methodology, has been 'settled' by assuming viscous damping although has been pointed out in the literature that in general it is not the case. The last two issues again are related to each other in the sense that for identification of the non-proportional damping parameters a reliable method of modal analysis is also required.

From the various studies reported in section 1.4 on modal analysis of non-classically damped systems, it seems that here has not been any single method which optimally uncouples the equations of motion over a wide range of different conditions (for example if

the modal damping matrix is not diagonally dominant or natural frequencies are not well separated, etc.). We have also seen that in general it is not possible to obtain an index of non-proportionality for a system since it in turn depends on excitation frequency. In summary it may be said that, unlike *the* traditional modal analysis method for proportionally damped systems, no such single method exists for non-proportionally damped systems. This demands new research in this area. In the present report we have considered the use of complex modes as an attempt to solve the problem.

Most of the techniques for detecting damping in a structure either consider the structure to be proportionally damped or *apriori* assumes some particular model of damping and tries to fit parameters in it with regard to some specific structure. This *apriori* selection of damping no doubt hides the physics of the system and there has not been any indication in the literature on how to find a damping model by doing conventional vibration testing. However another relevant question in this context is that if this *apriori* selection of damping model matters from an engineering point of view, it may be possible that a pre-assumed damping model with a correct set of parameters may represent the system response quite well, although the actual physical mechanism behind the damping may be different. These issues have been discussed in the present report. It has already been pointed out that, in conjunction with traditional experimental modal analysis based on real mode shapes, we can obtain the damping ratios for each mode considered in the analysis. This method may lead to acceptable proximity to the measured transfer functions with the reconstructed one, but fails to offer *any* indication of spatial distribution of damping in the structure whatsoever. Motivated by these existing gaps in the literature, a systematic study to detect the spatial distribution of damping in both continuous and discrete systems has been carried out in the next chapter of this report. In the last chapter a research project aimed to address the above mentioned issues has been proposed.

Chapter 2

IDENTIFICATION OF DAMPING

2.1 Introduction

In the last chapter it has been brought out that,in most realistic situations the damping in a vibrating structure will be non-proportional and thus the system will not possess classical normal modes. The proportional damping assumption is merely a mathematical convenience. In the presence of general damping, the mode shapes and the natural frequencies of a structure become complex. Recently Woodhouse (1998) has developed a methodology for evaluation of complex modes, natural frequencies and consequently the transfer functions of discrete systems with general linear damping models. In this chapter, this analysis is extended to distributed parameter systems and as an example applied to an axially vibrating rod. This method although can handle non-proportional damping models (with some small damping assumptions) within the scope of well known modal analysis methods but does not give any light into the kind of damping model to be used or spatial distribution of damping or even parameter values to be used in the equations of motion. It may be noted that due to the use of non-proportional damping models, the conventional way of *fixing* the damping values for a vibrating structure, such as percentage of critical damping, can no longer be used for analysis purposes as it does not make any sense in this context. So this method in turn also demands a more accurate description of damping in the structure. In this chapter a methodology for identification of the spatial distribution of damping using complex mode shapes and natural frequencies has been proposed. We also have tried to find an equivalent dissipation function for any kind of general damping present in the structure. With this fitted dissipation function and together with the approximate analysis methods developed earlier, the transfer functions are compared with the original transfer functions of the system. A discrete analogue of the axially vibrating rod, namely n spring-mass systems connected in series, has also been studied in this context to get more insight into this problem. Numerical examples for both the problems considered in this chapter bring out the different features associated with the methodology developed.

2.2 General Continuous System With Non-Proportional Damping

A linear damped continuous dynamic system in which the displacement variable $U(\mathbf{r},t)$, where $\mathbf{r}$ is the spatial position vector and t is time, specified in some domain $\mathcal{D}$, is governed by a linear partial differential equation

$$\rho(\mathbf{r})\frac{\partial^2 U(\mathbf{r},t)}{\partial t^2} + L_1\frac{\partial U(\mathbf{r},t)}{\partial t} + L_2 U(\mathbf{r},t) = p(\mathbf{r},t); \qquad \mathbf{r}\in\mathcal{D}, t\in[0,T] \tag{2.1}$$

with homogeneous linear boundary conditions of the form

$$M_1\frac{\partial U(\mathbf{r},t)}{\partial t} = 0; \quad M_2 U(\mathbf{r},t) = 0; \qquad \mathbf{r}\in\Gamma \tag{2.2}$$

specified on some boundary surface Γ. In the above equation $\rho(\mathbf{r})$ is the mass distribution of the system, $p(\mathbf{r},t)$ is the distributed time-varying forcing function, L_2 is the spatial self-adjoint stiffness operator. The damping operator L_1 can be written in the form

$$L_1\frac{\partial U(\mathbf{r},t)}{\partial t} = \int_{\mathcal{D}}\int_{-\infty}^{t} C_1(\mathbf{r},\xi,t-\tau)\frac{\partial U(\mathbf{r},t)}{\partial t}|_{(\xi,\tau)}\,\mathrm{d}\tau\,\mathrm{d}\xi \tag{2.3}$$

where $C_1(\mathbf{r},\xi,t)$ is the kernel function. It may be noted that the values of the variable $U(\mathbf{r},t)$ at different time instants and spatial locations are coupled through this kernel function. Kernel functions that serve similar purposes have been described by different names in different subjects, and different models have been used to describe them. In principle, any function which makes the rate of energy dissipation,

$$F(t) = \frac{1}{2}\int_{\mathcal{D}}\left\{\int_{\mathcal{D}}\int_{-\infty}^{t} C_1(\mathbf{r},\xi,t-\tau)\frac{\partial U(\mathbf{r},t)}{\partial t}|_{(\xi,\tau)}\mathrm{d}\tau\,\mathrm{d}\xi\right\}\frac{\partial U(\mathbf{r},t)}{\partial t}|_{(\mathbf{r},t)}\,\mathrm{d}\mathbf{r} \tag{2.4}$$

non-negative can be used for a kernel function. Equation (2.1) together with equation (2.3) represents a continuous dynamic system with general linear damping. It may be noted that if in equation (2.1) $L_1 = 0$, *i.e.* an undamped system, or if the system satisfies the criteria given by Caughey and O'Kelly (1965) then the system will possess classical normal modes. However, due to the general nature of the operator L_1 as described by equation (2.3), there is no definite reason why the system should have classical normal modes. Thus the mode shapes and natural frequencies of such system in general will be complex in nature. In this context we wish to note that the system expressed by (2.1) and the damping operator defined in (2.3) represents a partial integro-differential equation with the boundary conditions given in equation (2.2). A general eigenvalue solution of such a system is mathematically difficult and so some approximation of the kernel function $C_1(\mathbf{r},\xi,t)$ has been made based on the physical nature of the damping model considered in this study. In the first assumption we consider that the kernel function is delta related in space and time, that is

$$C_1(\mathbf{r},\xi,t-\tau) = C(\mathbf{r})\delta(\mathbf{r}-\xi)\delta(t-\tau). \tag{2.5}$$

This spatial delta function physically means that the damping force is 'locally reacting' and the time delta function implies that it depends only on the instantaneous value of the motion. From equation (2.4) the rate of energy dissipation leads to the familiar Rayleigh dissipation function defined by

$$F(t) = \frac{1}{2}\int_{\mathcal{D}} C(\mathbf{r}) \left(\frac{\partial U(\mathbf{r},t)}{\partial t}\right)^2 \mathrm{d}\mathbf{r} \tag{2.6}$$

So this model basically represents the well known 'viscous damping' model: however, no assumption on proportional damping will be made in this study. In the other assumption we consider that the kernel function is delta related in space but depends on the past time histories via a convolution integral as described by the equation (2.3), so the kernel takes form of

$$C_1(\mathbf{r},\xi,t-\tau) = g(\mathbf{r},t-\tau)\delta(\mathbf{r}-\xi). \tag{2.7}$$

This represents a locally reacting general damping model. In the following sections we consider these two damping models separately and derive expressions for complex mode shapes, natural frequencies and transfer functions. In both the formulations it has been assumed that the value of damping force is small compared to the stiffness and inertia forces.

2.2.1 Dissipation Function Model With Small Damping

The dissipation function model for continuous systems has been studied extensively in the literature using proportional damping assumption (for example see Meirovitch (1967), Paz (1985)). Combining equation (2.1), the damping operator (2.3) and the assumption described by equation (2.5), the equation of motion can be written as

$$\rho(\mathbf{r})\frac{\partial^2 U(\mathbf{r},t)}{\partial t^2} + C(\mathbf{r})\frac{\partial U(\mathbf{r},t)}{\partial t} + L_2 U(\mathbf{r},t) = p(\mathbf{r},t). \tag{2.8}$$

Assuming harmonic solutions for the linear problem $U(\mathbf{r},t) = \phi(\mathbf{r})\exp[\mathrm{i}\omega t]$ and substituting into the above equation, for free vibration we have

$$-\omega^2\rho(\mathbf{r})\phi(\mathbf{r}) + \mathrm{i}\omega C(\mathbf{r})\phi(\mathbf{r}) + L_2\phi(\mathbf{r}) = 0 \tag{2.9}$$

The undamped eigenvalue problem can be obtained by substituting $C(\mathbf{r}) = 0$ in the above equation: doing so one obtains

$$L_2\phi(\mathbf{r}) = \omega^2\rho(\mathbf{r})\phi(\mathbf{r}) \tag{2.10}$$

It is well known that in this case there exist a set of functions (mode shapes) $\phi_j(\mathbf{r})$ which satisfy the boundary condition on Γ having the following orthogonality properties

$$\begin{aligned} \int_{\mathcal{D}} \phi_j(\mathbf{r})\rho(\mathbf{r})\phi_k(\mathbf{r}) &= \delta_{jk} \\ \int_{\mathcal{D}} \phi_j(\mathbf{r})L_2\phi_k(\mathbf{r}) &= \omega_j^2\delta_{jk} \end{aligned} \tag{2.11}$$

where δ_{jk} is the Kroneker's delta function and ω_j are the natural frequencies of the system. Now it is common to assume that the mode shapes are simultaneously orthogonal to damping operator also and thus the mode shapes of damped system coincides with undamped mode shapes. However, here we are interested in the case where it is not possible to find a set of functions which will be simultaneously orthogonal to mass, stiffness and damping operators. In this case if the damping is small, the roots of equation (2.9), say $\bar{\omega}_n$, will be close to $\pm\omega_n$ for $n = 1, 2 \cdots \infty$ and the corresponding eigenfunctions, say $\bar{\phi}_n(\mathbf{r})$ are also expected to be close of $\phi_n(\mathbf{r})$. It should be noted that in general these quantities will be complex in nature. Let us try a solution of the form

$$\bar{\phi}_n(\mathbf{r}) = \sum_{j=1}^{\infty} \alpha_j \phi_j(\mathbf{r}); \qquad \text{where } \alpha_n = 1, \quad \| \alpha_j \| << 1 (j \neq n) \tag{2.12}$$

Substituting $\bar{\phi}_n(\mathbf{r})$ in place of $\phi_n(\mathbf{r})$ in equation (2.9), multiplying by $\phi_k(\mathbf{r})$ and carrying out the integration $\int_{\mathcal{D}} (\bullet)\, \mathrm{d}\mathbf{r}$ one obtains

$$-\omega^2 \alpha_k + \mathrm{i}\omega \sum_{j=1}^{\infty} \alpha_j C'_{kj} + \omega_k^2 \alpha_k = 0 \tag{2.13}$$

where

$$C'_{kj} = \int_{\mathcal{D}} \phi_k(\mathbf{r}) C(\mathbf{r}) \phi_j(\mathbf{r})\, \mathrm{d}\mathbf{r} \tag{2.14}$$

Now following Woodhouse (1998) the expressions for complex natural frequencies and mode shapes can be obtained as

$$\bar{\omega}_n \approx \pm\omega_n + \mathrm{i} C'_{nn}/2 \qquad \text{for } n = 1, 2, \cdots \infty \tag{2.15}$$

and

$$\bar{\phi}_n(\mathbf{r}) \approx \phi_n(\mathbf{r}) + \mathrm{i} \sum_{k=1, \neq n}^{\infty} \frac{\omega_n C'_{kn} \phi_k(\mathbf{r})}{\omega_n^2 - \omega_k^2} \qquad \text{for } n = 1, 2, \cdots \infty \tag{2.16}$$

In the above equations the complex nature of the solution arises due to the term C'_{kj} which represents damping function in modal space. If the undamped mode shapes are simultaneously orthogonal to the damping function then C'_{kj} reduces to Kroneker's delta function and the real undamped natural frequencies and modes shapes can be retrieved form equations (2.15) and (2.16). Thus as expected, the complex nature of the natural frequencies and mode shapes arises due to non-orthogonality of the undamped mode shapes over the damping function.

Transfer Function:
Assume the forcing function $p(\mathbf{r}, t)$ in equation (2.8) of the form $p(\mathbf{r}, t) = P\delta(\mathbf{r} - \mathbf{z}) \exp[\mathrm{i}\omega t]$ denoting a point harmonic load at a location $\mathbf{z}$. Now the transfer function for the continuous system, $H(\mathbf{r}, \mathbf{z}, \omega)$, can be obtained by evaluating the displacement at some other point $\mathbf{r}$ and dividing it by the force in the frequency domain. Express the response as

$$U(\mathbf{r}, t) = \sum_{j=1}^{\infty} q_j \phi_j(\mathbf{r}) \exp[\mathrm{i}\omega t] \tag{2.17}$$

Substituting $p(\mathbf{r},t)$, $U(\mathbf{r},t)$ in equation (2.8), multiplying by $\phi_k(\mathbf{r})$ and carrying out the operation $\int_{\mathcal{D}}(\bullet)\,\mathrm{d}\mathbf{r}$ gives

$$-\omega^2 q_k + \mathrm{i}\omega\sum_{j=1}^{\infty} q_j C'_{kj} + \omega_k^2 q_k = P\phi_k(\mathbf{z}) \tag{2.18}$$

Now following the method outlined by Woodhouse (1998), the transfer function up to the first order approximation can be expressed as

$$H(\mathbf{r},\mathbf{z},\omega) \approx \sum_{k=1}^{\infty}\frac{1}{2\omega_k}\left\{-\frac{\bar{\phi}_k(\mathbf{r})\bar{\phi}_k(\mathbf{z})}{\omega-\bar{\omega}_k} + \frac{\bar{\phi}_k^*(\mathbf{r})\bar{\phi}_k^*(\mathbf{z})}{\omega+\bar{\omega}_k^*}\right\} \tag{2.19}$$

with $(.)^*$ denoting the complex conjugate. The above expressed transfer function uses only complex modes and natural frequencies derived earlier. This transfer function can be viewed as a generalisation of the well known proportionally damped transfer function for continuous systems. For all practical purposes of calculation, the infinite sums in equation (2.19) and also in equation (2.16) can be truncated to a finite value by retaining a finite number of mode shapes.

2.2.2 General Locally Reacting Damping Models

For this kind of damping model the kernel function takes the form of that expressed by equation (2.7). Such damping models are also called as 'time hysteresis' damping (Banks and Inman, 1991) and most commonly associated with sinusoidal loading. Physically this kind of model represents that the damping force is dependent on the past time histories through a convolution integral over the kernel function. At some instant of time the total force contributing for energy dissipation, $Q(\mathbf{r},t)$, at a point $\mathbf{r}$ of the structure can be obtained as

$$\begin{aligned} Q(\mathbf{r},t) &= -\int_{\mathcal{D}}\int_{-\infty}^{t} C_1(\mathbf{r},\xi,t-\tau)\frac{\partial U(\mathbf{r},t)}{\partial t}|_{(\xi,\tau)}\,\mathrm{d}\tau\,\mathrm{d}\xi \\ &= -\int_{\mathcal{D}}\int_{-\infty}^{t} g(\mathbf{r},t-\tau)\delta(\mathbf{r}-\xi)\frac{\partial U(\mathbf{r},t)}{\partial t}|_{(\xi,\tau)}\,\mathrm{d}\tau\,\mathrm{d}\xi \\ &= -\int_{-\infty}^{t} g(\mathbf{r},t-\tau)\frac{\partial U(\mathbf{r},t)}{\partial t}\mathrm{d}\tau \end{aligned} \tag{2.20}$$

The negative sign is used only for mathematical convenience: this later will give rise to a positive sign for energy dissipation. The choice of $\dfrac{\partial U(\mathbf{r},t)}{\partial t}$ as *the* state variable responsible for energy dissipation is also used for our familiarity with the traditional 'dash-pot' models. However it must be noted that in principle any state variable can contribute to the energy dissipation and that exactly which state variable contributes and how is not very clear to us. So the damping models we have used here can be viewed as a spatial distribution of dash-pots

with a memory in it. Now the rate of energy dissipation is given by

$$\begin{aligned} F(t) &= -\frac{1}{2}\int_{\mathcal{D}} Q(\mathbf{r},t)\frac{\partial U(\mathbf{r},t)}{\partial t}\,\mathrm{d}\mathbf{r} \\ &= \frac{1}{2}\int_{\mathcal{D}}\left\{\int_{-\infty}^{t} g(\mathbf{r},t-\tau)\left(\frac{\partial U(\mathbf{r},t)}{\partial t}\right)^2 \mathrm{d}\tau\right\}\mathrm{d}\mathbf{r} \end{aligned} \tag{2.21}$$

It will be easier for further analysis to convert the above equation in to the frequency domain: doing so one obtains

$$F(\omega) = \frac{\omega^2}{2}\Re\left[\int_{\mathcal{D}} U^*(\mathbf{r},\omega)G(\mathbf{r},\omega)U(\mathbf{r},\omega)\,\mathrm{d}\mathbf{r}\right] \tag{2.22}$$

where $\Re(\bullet)$ represents real part $(\bullet)$ and $G(\mathbf{r},\omega)$ is the Fourier transform of the kernel function $g(\mathbf{r},t)$. For a physically realistic model of damping, $F(\omega)$ should be non-negative for all ω. This gives restriction on the kernel function and expressed as below.

Condition: *For a physically realistic model of damping, the integral of the real part of the Fourier transform of kernel function over the domain should be non-negative within the driving frequency range, or mathematically* $\int_{\mathcal{D}}\Re[G(\mathbf{r},\omega)]\,\mathrm{d}\mathbf{r} \geq 0$ *for all* ω.
This can be easily proved from equation (2.22) as follows. For a physically realistic model of damping we should have

$$\begin{aligned} F(\omega) &\geq 0 \\ \text{or } \frac{\omega^2}{2}\Re\left[\int_{\mathcal{D}} U^*(\mathbf{r},\omega)G(\mathbf{r},\omega)U(\mathbf{r},\omega)\,\mathrm{d}\mathbf{r}\right] &\geq 0 \\ \text{or } \frac{\omega^2}{2}\Re\left[\int_{\mathcal{D}} G(\mathbf{r},\omega)\mid U(\mathbf{r},\omega)\mid^2\,\mathrm{d}\mathbf{r}\right] &\geq 0 \\ \text{implies } \int_{\mathcal{D}}\Re[G(\mathbf{r},\omega)]\,\mathrm{d}\mathbf{r} &\geq 0 \end{aligned} \tag{2.23}$$

since for a real value of driving frequency $\omega^2 \geq 0$ and $\Re \mid U(\mathbf{r},\omega)\mid^2 \geq 0$.

Now assuming a harmonic solution for this linear problem, $U(\mathbf{r},t) = \varphi(\mathbf{r})\exp[\mathrm{i}\omega t]$, the equation of motion in the frequency domain can be expressed as

$$-\omega^2\rho(\mathbf{r})\varphi(\mathbf{r}) + \mathrm{i}\omega G(\mathbf{r},\omega)\varphi(\mathbf{r}) + L_2\varphi(\mathbf{r}) = 0 \tag{2.24}$$

Further, following the similar procedure outlined in the previous section we can have

$$-\omega^2\alpha_k + \mathrm{i}\omega\sum_{j=1}^{\infty}\alpha_j G'_{kj}(\omega) + \omega_k^2\alpha_k = 0 \tag{2.25}$$

with

$$G'_{kj}(\omega) = \int_{\mathcal{D}}\varphi_k(\mathbf{r})G(\mathbf{r},\omega)\varphi_j(\mathbf{r})\,\mathrm{d}\mathbf{r} \tag{2.26}$$

where $\varphi_j(\mathbf{r})$ are the undamped mode shapes. The analysis which follows is very much similar to that developed by Woodhouse (1998) and here we summarise only the results. The complex natural frequencies and mode shapes can be obtained as

$$\bar{\omega}_n \approx \pm\omega_n + \mathrm{i}G'_{nn}(\omega_n)/2 \qquad \text{for } n = 1, 2, \cdots \infty \tag{2.27}$$

and

$$\bar{\varphi}_n(\mathbf{r}) \approx \varphi_n(\mathbf{r}) + \mathrm{i}\sum_{k=1,\neq n}^{\infty} \frac{\omega_n G'_{kn}(\omega_n)\varphi_k(\mathbf{r})}{\omega_n^2 - \omega_k^2} \qquad \text{for } n = 1, 2, \cdots \infty \tag{2.28}$$

As in general $G'_{kj}(\omega_j)$ is complex in nature, unlike the previous case the real part of natural frequencies and mode shapes do not coincide with the undamped ones. Later in section 2.3 these issues will be discussed in more detail. Finally the transfer function can be obtained as

$$\mathcal{H}(\mathbf{r}, \mathbf{z}, \omega) \approx \sum_{k=1}^{\infty} \frac{1}{2\omega_k} \left\{ -\frac{R_k(\mathbf{r}, \mathbf{z})}{\omega - \bar{\omega}_k} + \frac{R_k^*(\mathbf{r}, \mathbf{z})}{\omega + \bar{\omega}_k^*} \right\} \tag{2.29}$$

where

$$R_k(\mathbf{r}, \mathbf{z}) \approx -\left\{ \varphi_k(\mathbf{r}) + \mathrm{i}\sum_{j=1,\neq k}^{\infty} \frac{\omega_k G'_{kj}(\omega_k)\varphi_j(\mathbf{r})}{\omega_k^2 - \omega_j^2} \right\} \left\{ \varphi_k(\mathbf{z}) + \mathrm{i}\sum_{j=1,\neq k}^{\infty} \frac{\omega_k G'_{jk}(\omega_k)\varphi_j(\mathbf{z})}{\omega_k^2 - \omega_j^2} \right\} \tag{2.30}$$

An interesting point to be noted is that this transfer function is not necessarily reciprocal. This is because different rows of G' matrix are calculated at different natural frequencies, and in general $G'_{jk}(\omega_k) \neq G'_{kj}(\omega_j)$.

2.2.3 Example: Axially Vibrating Rod

To illustrate the use of the expressions developed in the last section, the example of an axially vibrating rod will be considered. Figure 2.1 shows the example together with the numerical values considered. The equation of motion for free vibration of the rod of length L with constant mass per unit length ρ, and axial stiffness AE having general linear damping can be expressed as

$$\rho\frac{\partial^2 U(x,t)}{\partial t^2} = AE\frac{\partial^2 U(x,t)}{\partial x^2} + \int_{-\infty}^{t} g(x, t-\tau)\frac{\partial U(x,t)}{\partial t}\,|_{(x,\tau)}\,\mathrm{d}\tau \tag{2.31}$$

The boundary condition is considered as 'fixed-free', *i.e.* $U(0,t) = 0$ and $\dfrac{\partial U(x,t)}{\partial x}|_{(L,t)} = 0$. The undamped mode shapes can be obtained as

$$\begin{aligned} \varphi_j(x) &= \sqrt{\frac{2}{\rho L}}\sin(2j-1)\frac{\pi x}{2L} \\ \omega_j &= (2j-1)\frac{\pi}{2L}\sqrt{\frac{AE}{\rho}} \end{aligned} \tag{2.32}$$

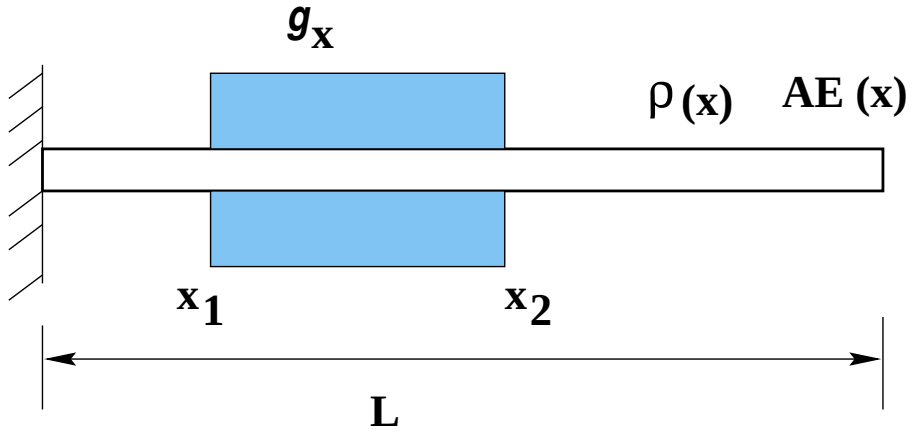

Figure 2.1: Axially vibrating rod, $\rho = 3.12\,Kg/m$, $AE = 80.0 \times 10^6\,N/m^2$, $L = 2\,m$, $x_1 = 0.5\,m$, $x_2 = 1.1\,m$

The damping model $g(x,t)$ is considered as a constant times a function of time between x_1 and x_2, *i.e.*, $g(x,t) = g_x g_t(t)$; $x_1 < x < x_2$ and for all t. This in turn means that we have considered a uniformly distributed damping of the form $g_x g_t(t)$ in between $x_1 < x < x_2$. In this chapter three different models of $g_t(t)$ have been considered
MODEL 1:

$$g_t(t) = \begin{cases} g_x & (0 < t < t_1) \\ 0 & (t_1 < t) \end{cases} \tag{2.33}$$

MODEL 2:

$$g_t(t) = g_x \exp[-\lambda t] \tag{2.34}$$

MODEL 3:

$$g_t(t) = \begin{cases} \dfrac{g_x}{2}\left[1 + \cos\left(\dfrac{\pi t}{t_3}\right)\right] & (0 < t < t_3) \\ 0 & (t_3 < t) \end{cases} \tag{2.35}$$

where t_1, λ and t_3 are constants. Figure 2.2 shows the plots of the three damping functions for some typical values of these parameters. The values of the constants t_1, λ, t_3 and g_x have been selected in such a way that the area under the respective curves approaches to the same constant value as $t \to \infty$. The area under these three damping functions can respectively be represented as $A_1 = g_x t_1$, $A_2 = \dfrac{g_x}{\lambda}$ and $A_3 = \dfrac{g_x t_3}{2}$. The numerical values of the constant area for all three damping models, say $A_{(k)}$, have been obtained by taking the damping factor $\zeta = 2\%$ at the k-th mode when the rod is proportionally damped over the whole length, *i.e.*, $A_{(k)} = 2\rho\zeta\omega_k \left(\dfrac{L}{x_2 - x_1}\right)$. Introduction of these different models physically means that

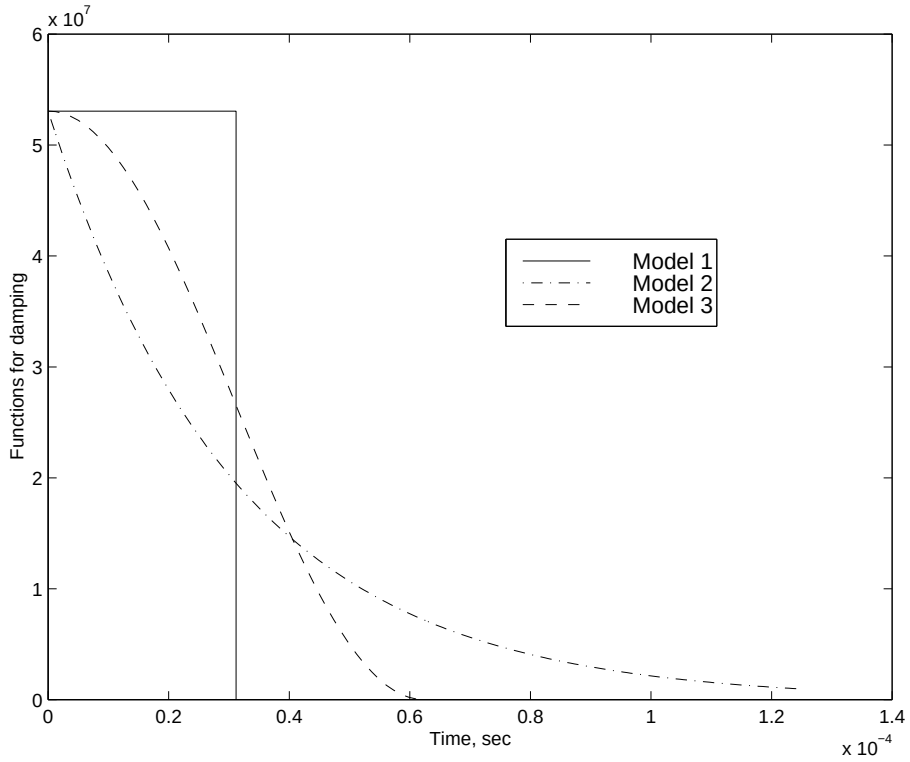

Figure 2.2: three different damping models for parameter set 1

the same amount of damping is redistributed in space and time in different ways. From the equations of the areas of the damping functions it may be observed that even after choosing a fixed value of area, there is no unique way one can select the values of the constants g_x, t_1, λ and t_3. Another condition of selecting these values will come from the *condition* of a physically acceptable damping model given by equation (2.23). However, model 2 is different than the other two models in the sense that for any given real frequency value, the real part of its Fourier transform never becomes negative and thus any range of parameter values can be chosen. Considering all the above facts we have selected the parameters of the following form

$$g_x = A_{(k)}^{1+s};\ t_1 = \frac{1}{A_{(k)}^{s}};\ \lambda = A_{(k)}^{s} \text{ and } t_3 = \frac{2}{A_{(k)}^{s}}$$

so that area under all the damping curves remains $A_{(k)}$. For further numerical experiments two different sets of values which will be of interest to us have been considered:

- Parameter Set 1: $k = 1$, $s = 1.3$
- Parameter Set 2: $k = 3$, $s = 2$

For the example considered here, the entries of the matrix $\mathbf{G}'(\omega)$ can be obtained as

$$G'_{kj}(\omega) = g_x \int_{x_1}^{x_2} \varphi_k(x) G_\omega(\omega) \varphi_j(x)\, \mathrm{d}x \tag{2.36}$$

where $G_\omega(\omega)$ is the Fourier transform of $g_t(t)$. Now application of equation (2.27) and (2.28) directly gives the complex natural frequencies and mode shapes. The real part of the complex mode shapes are very similar in nature to that of the undamped mode shapes. Figure 2.3

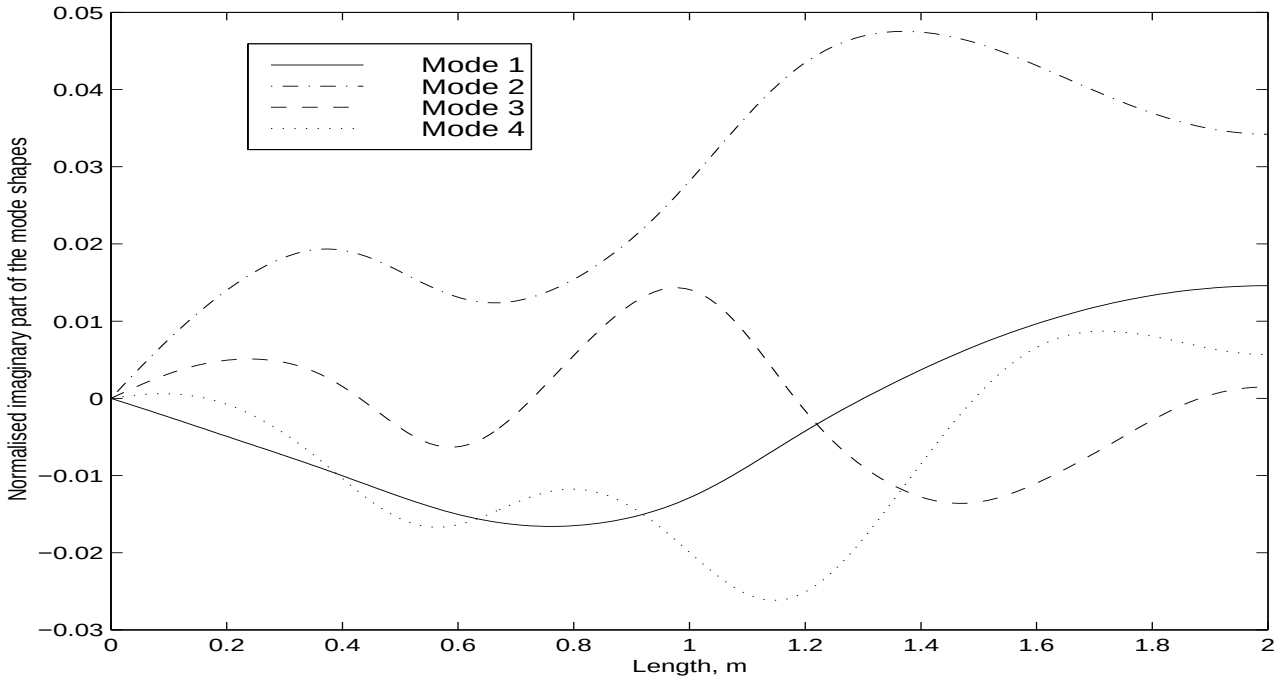

Figure 2.3: Normalised imaginary part of first four modes, damping model 3, parameter set 1

and 2.4 shows the imaginary part of the first four mode shapes using damping model 3 for parameter set 1 and 2 respectively. This mode shapes are normalised with the maximum value of the real part of the complex modes, *i.e.* we have plotted $\dfrac{\Im\{\varphi_k(x)\}}{\sqrt{\dfrac{2}{\rho L}}}$, for $k = 1 \cdots 4$. It may be observed that the imaginary part of the mode shapes do not have much similarity with the real part of it, for example with parameter set 1, the fourth mode does not have three zeros while instead of two zeros third mode have four zeros. From figure 2.3 we observe that, with parameter set 1, the imaginary part of the mode shapes are about 5% of the real part of it, while from figure 2.4, that with parameter set 2 is about 25%. This can be explained form the Q-factors of the system for the respective parameter sets. The Q-factors for the first five modes are tabulated in Table 2.1 for both the parameter sets. It can be seen that

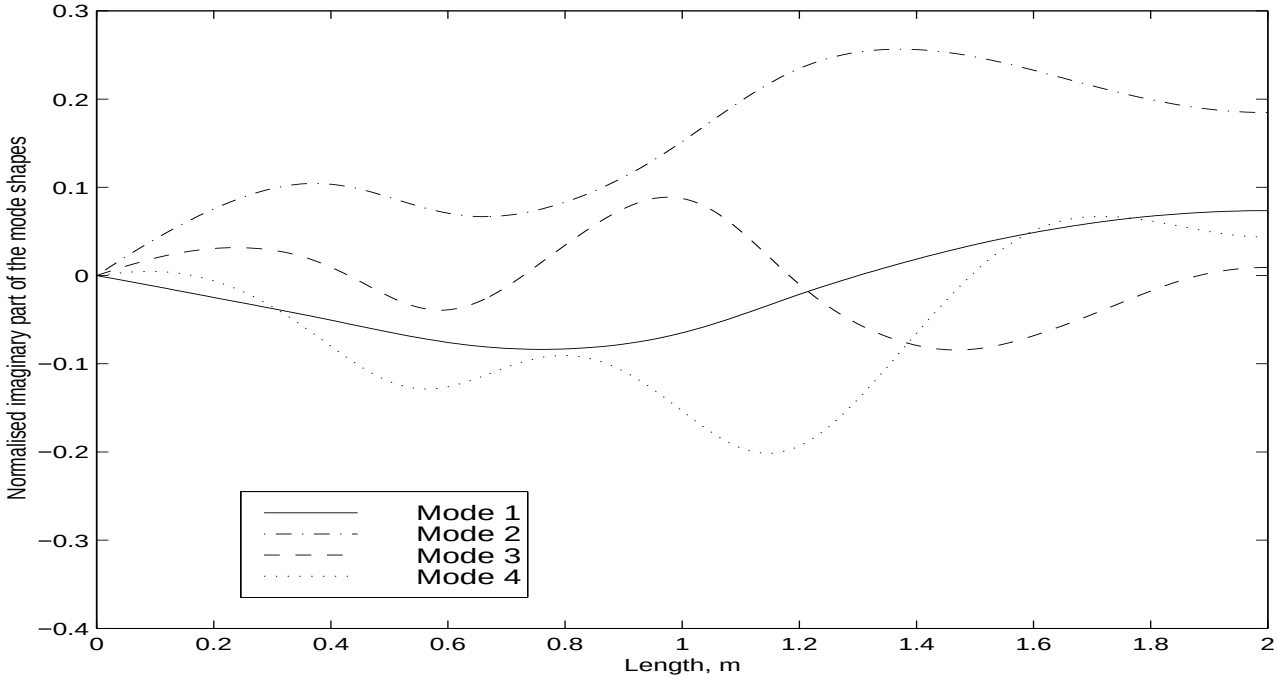

Figure 2.4: Normalised imaginary part of first four modes, damping model 3, parameter set 2

the Q-factors are comparatively large for parameter set 1 indicating less damping compared to that with parameter set 2. This fact has been reflected by the normalised plots of the imaginary parts of the complex modes-shapes.

	Parameter Set 1			**Parameter Set 2**		
Mode No	Model 1	Model 2	Model 3	Model 1	Model 2	Model 3
1	23.0322	23.7349	23.1196	4.5638	4.5639	4.5638
2	32.5306	40.1747	33.4880	6.1433	6.1433	6.1433
3	131.9431	207.7372	142.5974	22.8974	22.8975	22.8974
4	154.9204	302.3536	180.5681	23.3312	23.3314	23.3313
5	220.2363	491.0387	284.5945	27.0879	27.0882	27.0879

Table 2.1: Q-factors for the first 5 mode shapes for the three damping models

Using the complex natural frequencies and mode shapes the transfer functions can be calculated from equation (2.29). Figure 2.5 and 2.6 shows the transfer function $\mathcal{H}(x, z, \omega)$, at $x = 0.75$ and $z = 1.6$ for all the 3 damping models with the two sets of values considered here. For parameter set 1 the transfer functions are very much similar for all the three

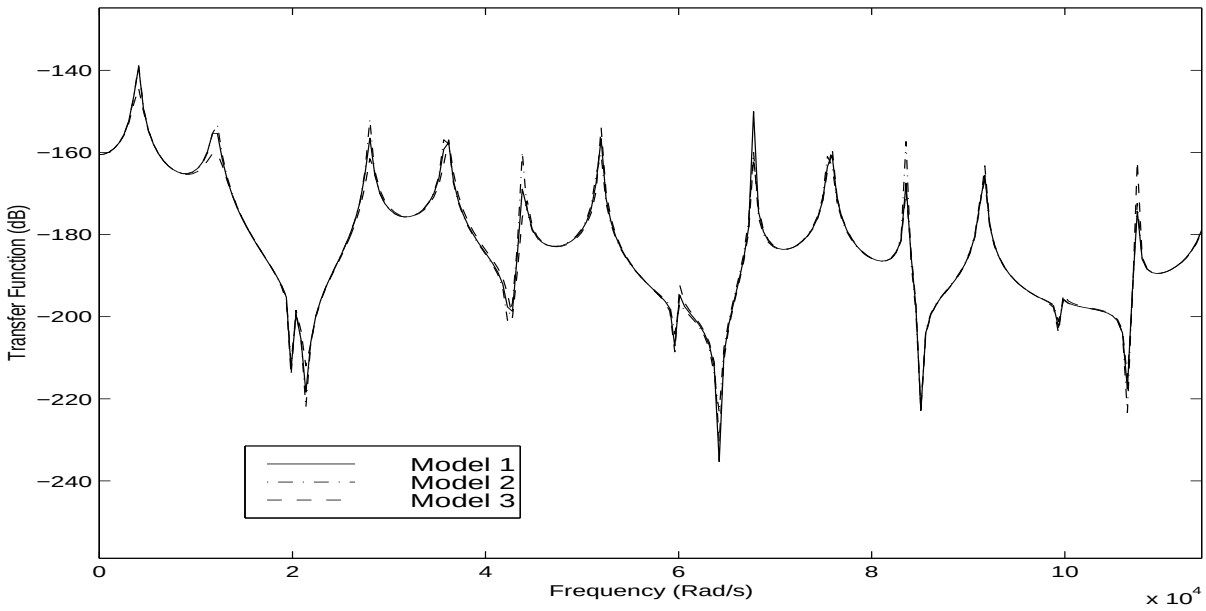

Figure 2.5: Transfer function $\mathcal{H}(x, z, \omega)$ for all the damping models at the points $x = 0.75$ and $z = 1.6$, parameter set 1

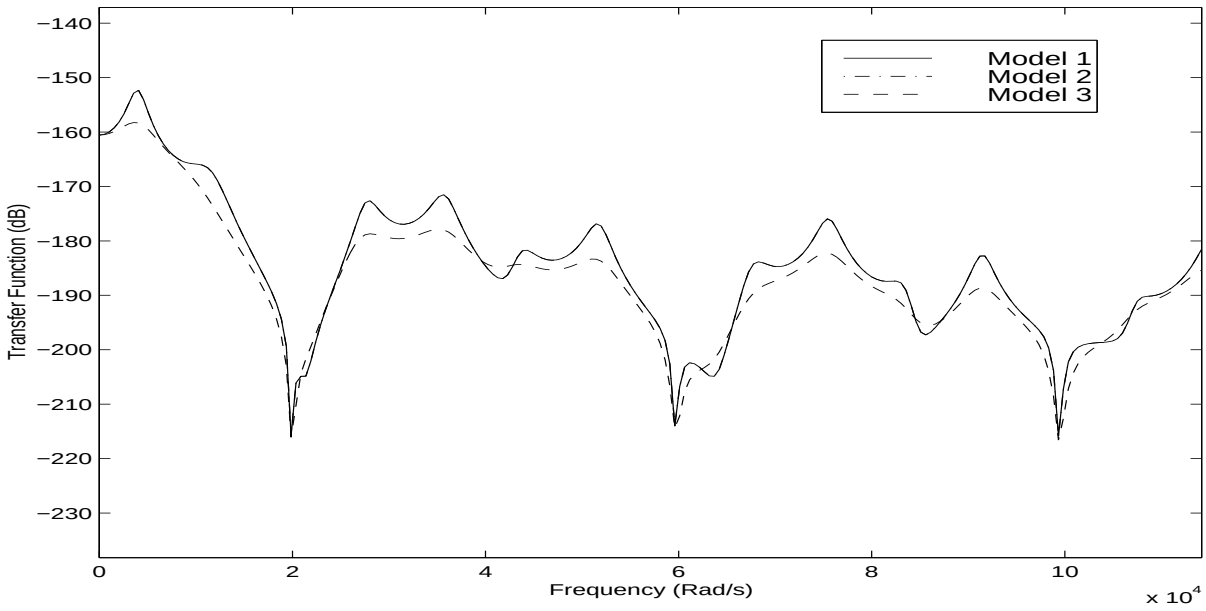

Figure 2.6: Transfer function $\mathcal{H}(x, z, \omega)$ for all the damping models at the points $x = 0.75$ and $z = 1.6$, parameter set 2

damping models whereas for parameter set 2, model 1 and 2 appears to be very much similar but model 3 predicts different (lower) result. It should be remembered that for both the cases the area under the function $g_t(t)$ is same for the different damping models.

It may be of interest to us to understand the effect of the Q-factors on these results. So, for the parameter set 1, when the Q-factors are comparatively higher than that of parameter set 2, the transfer functions for all the damping models remain the same. For a comparatively low value of Q-factors, as in the case of parameter set 2, the transfer function using model 3 predicts less value that that of the other two models. Finally, form the figure 2.5, it is interesting to note that the transfer function calculated with three different damping models give rise to very much similar result. In the light of this fact it can be concluded that, looking at the transfer functions, in general, it is not possible to detect the underlying damping mechanisms.

2.3 Identification of Spatial Distribution of Damping

Most of the general methods for evaluation of the damping parameters use the proportional damping assumption. In this case it is possible to find out the modal damping parameters in conjunction with experimental modal analysis. The usual procedure for doing this (Ewins, 1984) can be described as follows :

1. measure a set of transfer functions $H_{ij}(\omega)$ by hitting an impulse hammer at different grid points of a structure
2. obtain the natural frequencies ω_n by pole fitting method
3. evaluate the modal bandwidth parameter $\Delta\omega_n$ from the frequency response function, then the Q-factor $Q_n = \frac{\omega_n}{\Delta\omega_n}$ and from it the modal damping factor $\xi_n = \frac{1}{2Q_n}$
4. determine the modal amplitude factors a_n to obtain the mode shapes, $u_n(x)$
5. finally reconstruct the transfer function using the well known formula

$$H'(x, y, \omega) = \sum_{n=1}^{N} \frac{u_n(x)u_n(y)}{\omega_n^2 + \mathrm{i}\Delta\omega_n - \omega^2} \tag{2.37}$$

to verify the accuracy of the evaluated parameters. In the above expression N indicates number of modes included in the analysis.

It can be clearly observed from the above procedure that it is not possible to find out the spatial distribution of damping though the reconstructed transfer functions may match well with the measured ones. Here we propose a method to find out the spatial distribution of damping within the scope of experimental modal analysis. This method is based on fitting an approximate dissipation function model to the measured data and can be done as follows:

1. measure a set transfer functions $H_{ij}(\omega)$ by hitting an impulse hammer at different grid points of a structure

2. determine the complex natural frequencies $\bar{\omega}_n$ and complex mode shapes $\bar{\phi}_n$

3. use equation (2.15), real part of $\bar{\omega}_n$ are the undamped natural frequencies, $\omega_n = \Re(\bar{\omega}_n)$. From the imaginary part get the diagonal terms of the modal damping matrix, $C'(n,n) = 2\Im(\bar{\omega}_n)$.

4. consider the complex mode shapes $\bar{\phi}_n$ and use equation (2.16): the real part of $\bar{\phi}_n$ is the undamped mode shape, *i.e.* $\phi_n = \Re(\bar{\phi}_n)$. The off-diagonal terms of the modal damping matrix C'_{kj}, $j \neq k$ can be obtained from the imaginary parts of $\bar{\phi}_n$,

5. from the last two steps we have the full damping matrix $\mathbf{C}'$ in the modal coordinates, transforming it back to the original coordinate will give the spatial distribution of the damping in the structure.

6. finally reconstruct the transfer functions using equation (2.19) for checking.

An important issue here is that of symmetry. Only if the measured transfer functions are symmetric we can hope to fit a dissipation function model with the measured data. In the initial stage some analytical study is needed to verify the proposed method for detecting the spatial distribution damping. So, instead of doing experiments on a real structure, the complex natural frequencies and mode shape data are generated using the general damping models outlined in section 2.2.2. Our approach towards verifying the proposed method is to introduce a localised damping in some portion of the structure and then try to detect it by the procedure outlined above. For numerical examples the problems of the axially vibrating rod considered in section 2.2.3 and a linear n-DOF chain has been taken.

2.4 Fitting Dissipation Function Model to The General damping Model

2.4.1 Continuous System

Approximate complex natural frequencies and mode shapes for a system governed by a locally reacting general linear damping model can be obtained from the expressions given in equations (2.27) and (2.28). Use the following notation

$$u_n(\mathbf{r}) = \Re[\bar{\varphi}_n(\mathbf{r})]; \qquad v_n(\mathbf{r}) = \Im[\bar{\varphi}_n(\mathbf{r})]; \tag{2.38}$$

From the above equation, $u_n(\mathbf{r})$ have been taken as the undamped mode shapes of the system for which the dissipation function to be fitted. It should be noted that since $G'_{kn}(\omega_n)$ in equation (2.28) is complex, $u_n(\mathbf{r})$ are not necessarily similar to the undamped modes shapes of the original structure we have started with. For the same reason, the natural frequencies

obtained by taking the real part of the complex natural frequencies, $\omega_n = \Re(\bar{\omega}_n)$, are also not same with that of the original system. This perhaps demands updating of the mass and stiffness properties of the system. However, in this introductory study these issues have not been considered. This problem we have partly tackled in another way by allowing the undamped mode shapes are not to be exactly orthogonal with respect to mass, *i.e.* it does not satisfy the properties described by equations (2.11).

Now consider equation (2.16), with regards to the notations described in equation (2.38) $u_n(\mathbf{r}) = \phi_n(\mathbf{r})$. If a dissipation function has to be fitted then the complex mode shapes should match with the complex mode shapes of the system with general linear damping, *i.e.* we should have

$$\bar{\phi}_n(\mathbf{r}) = u_n(\mathbf{r}) + \mathrm{i}v_n(\mathbf{r}) \tag{2.39}$$

But it can be seen from equation (2.16) that the imaginary part of $\bar{\phi}_n(\mathbf{r})$ should be a linear combination of $u_n(\mathbf{r})$, say

$$v_n(\mathbf{r}) = \sum_{k=1}^{\infty} B_{kn} u_k(\mathbf{r}); \qquad \text{where } B_{kn} = \frac{\omega_n C'_{kn}}{\omega_n^2 - \omega_k^2} \tag{2.40}$$

The constants B_{kn} should be calculated such that the error in representing $v_n(\mathbf{r})$ by such a sum is minimised. It may be noted that in the above sum we have considered the $k = n$ term although in the original sum in equation (2.16) this term has been disregarded. This is done to ease the mathematical formulation to be followed and has no effect on the result. Our interest lies in calculating C'_{kn} from B'_{kn} through the relationship given by the second part of the equation (2.40), and indeed for $k = n$ we obtain $C'_{kn} = 0$. The diagonal terms C'_{nn} are instead obtained from the imaginary part of the complex natural frequencies as

$$C'_{nn} = 2\Im(\bar{\omega}_n) \tag{2.41}$$

The error from representing $v_n(\mathbf{r})$ by the series sum in equation (2.40) can be expressed as

$$\xi_n(\mathbf{r}) = v_n(\mathbf{r}) - \sum_{k=1}^{\infty} B_{kn} u_n(\mathbf{r}) \tag{2.42}$$

For minimising the error a Galerkin kind of approach (see Zienkiewicz and Morgan, 1982) has been adopted here. The undamped mode shapes $u_l(\mathbf{r})$; $l = 1, 2 \cdots \infty$, are taken as 'weighting functions'. Now using the Galerkin method on $\xi_n(\mathbf{r})$ for a fixed n one obtains

$$\int_{\mathcal{D}} \xi_n(\mathbf{r}) u_l(\mathbf{r}) \mathrm{d}\mathbf{r} = 0; \qquad l = 1, 2, \cdots \infty \tag{2.43}$$

Using the notation $\int_{\mathcal{D}}(\bullet)\mathrm{d}\mathbf{r} = <\bullet>$ and combining equations (2.42) and (2.43) gives

$$\begin{aligned} \left\langle \left\{ v_n(\mathbf{r}) - \sum_{k=1}^{\infty} B_{kn} u_k(\mathbf{r}) \right\} u_l(\mathbf{r}) \right\rangle &= 0 \\ \text{or} \quad \sum_{k=1}^{\infty} B_{kn} \left\langle u_k(\mathbf{r}) u_l(\mathbf{r}) \right\rangle &= \left\langle v_n(\mathbf{r}) u_l(\mathbf{r}) \right\rangle \\ \text{or} \quad \sum_{k=1}^{\infty} B_{kn} T_{kl} &= S_{ln}; \qquad l = 1, 2, \cdots \infty \end{aligned} \tag{2.44}$$

with $T_{kl} = \langle u_k(\mathbf{r}) u_l(\mathbf{r}) \rangle$ and $S_{ln} = \langle v_n(\mathbf{r}) u_l(\mathbf{r}) \rangle$. For purposes of calculation retaining a finite number of modes, N, equation (2.44) reads

$$\sum_{k=1}^{N} T_{kl} B_{kn} = S_{ln}; \qquad l = 1, 2, \cdots N \tag{2.45}$$

Since T_{kl} is $n-$independent for all $n = 1, 2, \cdots N$ the above equation can be cast in a matrix form

$$\mathbf{TB} = \mathbf{S} \tag{2.46}$$

where $\mathbf{T}_{N\times N} = \mathbf{U}^t\mathbf{U}$ and $\mathbf{S}_{N\times N} = \mathbf{U}^t\mathbf{V}$ with superscript $(\bullet)^t$ denoting the matrix transpose. The terms

$$\begin{aligned} \mathbf{U} &= [u_1(\mathbf{r}), u_2(\mathbf{r}), \cdots u_N(\mathbf{r})]_{1\times N} \\ \mathbf{V} &= [v_1(\mathbf{r}), v_2(\mathbf{r}), \cdots v_N(\mathbf{r})]_{1\times N} \end{aligned} \tag{2.47}$$

are the matrices with real and imaginary part of the complex mode shapes of the original system with general linear damping. So from equation (2.46) the matrix of constants $\mathbf{B}_{N\times N}$ can be obtained as

$$\mathbf{B} = \mathbf{T}^{-1}\mathbf{S} \tag{2.48}$$

and from this the coefficients of the modal damping matrix can be derived as

$$C'_{kn} = \frac{(\omega_n^2 - \omega_k^2) B_{kn}}{\omega_n}; \qquad \text{for } k = n = 1, 2 \cdots N; k \neq n \tag{2.49}$$

The above two equations together with equation (2.41) completely define the modal damping matrix $\mathbf{C}'$. It is easy to notice from the above equations that we need only the complex natural frequencies and mode shapes to obtain $\mathbf{C}'$. The damping in the original coordinates can now be obtained as

$$c(\mathbf{r}, \mathbf{z}) = \sum_{i=1}^{N} \sum_{j=1}^{N} u_i(\mathbf{r}) C'_{ij} u_j(\mathbf{z}) \tag{2.50}$$

It is interesting to notice that through the above transformation in general we will obtain a non-locally reacting damping model although we have started with a locally reacting model. If $c(\mathbf{r}, \mathbf{z})$ turns out to be large in the domain $\mathbf{r} = \mathbf{z}$ compared to $\mathbf{r} \neq \mathbf{z}$ the fitting can be regarded as satisfactory. In the numerical examples later these issues of fitting have been considered in more detail.

2.4.2 Discrete Systems

For a discrete system with N degree of freedom the analysis remains very much the same as that of the continuous system described above. The only difference occurs in that the B_{kn} can be evaluated exactly without going through the Galerkin kind of error minimisation

scheme. So for a discrete system with the real and imaginary part of the eigenvectors being $\mathbf{u}_{n_{N\times 1}}$ and $\mathbf{v}_{n_{N\times 1}}$ equation (2.40) can be modified to read

$$\mathbf{v}_n = \sum_{k=1}^{\infty} B_{kn}\mathbf{u}_n \tag{2.51}$$

For all $n = 1, 2, ..N$ the above equation can simply be cast in a matrix form as

$$\mathbf{UB} = \mathbf{V}; \qquad \mathbf{B} = \mathbf{U}^{-1}\mathbf{V} \tag{2.52}$$

with

$$\begin{aligned} \mathbf{U} &= [\mathbf{u}_1, \mathbf{u}_1, \cdots \mathbf{u}_N]_{N\times N} \\ \mathbf{V} &= [\mathbf{v}_1, \mathbf{v}_1, \cdots \mathbf{v}_N]_{N\times N} \end{aligned} \tag{2.53}$$

Obtaining $\mathbf{C}'$ using (2.49) the damping matrix in original spatial coordinates can now be obtained as

$$\mathbf{c} = \mathbf{U}^t\mathbf{C}'\mathbf{U} \tag{2.54}$$

It is interesting to note that application of the Galerkin method of error minimisation for discrete systems, although not necessarily required, gives the exact result given by equation (2.52). Starting from equation (2.48) this can be verified easily as follows :

$$\mathbf{B} = \mathbf{T}^{-1}\mathbf{S} = \left[\mathbf{U}^t\mathbf{U}\right]^{-1}\left[\mathbf{U}^t\mathbf{V}\right] = \mathbf{U}^{-1}\mathbf{U}^{t^{-1}}\mathbf{U}^t\mathbf{V} = \mathbf{U}^{-1}\left[\mathbf{U}\mathbf{U}^{-1}\right]^t\mathbf{V} = \mathbf{U}^{-1}\left[\mathbf{I}\right]^t\mathbf{V} = \mathbf{U}^{-1}\mathbf{V} \tag{2.55}$$

which is exactly same expression as described in equation (2.52).

2.4.3 General Method

In view of the results obtained from the above two sections now we can unify the method for detection of the spatial distribution of damping for both continuous and discrete systems. The expressions in the last two sections although developed for fitting a dissipation function model to a general damping model, could also be used in the context of experimental modal analysis. In summary, this procedure can be described by the following steps

1. measure a set of transfer functions $H_{ij}(\omega)$ by hitting an impulse hammer at different grid points of a structure
2. determine all the complex natural frequencies $\bar{\omega}_n$ and complex mode shapes $\bar{\phi}_n$ from the transfer function, obtain the complex mode shape matrix $\bar{\mathbf{\Phi}}$
3. evaluate the 'undamped natural frequencies' as $\omega_n = \Re(\bar{\omega}_n)$.
4. set $\mathbf{U} = \Re\left[\bar{\mathbf{\Phi}}\right]$ and $\mathbf{V} = \Im\left[\bar{\mathbf{\Phi}}\right]$, form these obtain $\mathbf{T} = \mathbf{U}^t\mathbf{U}$ and $\mathbf{S} = \mathbf{U}^t\mathbf{V}$. Now denote $\mathbf{B} = \mathbf{T}^{-1}\mathbf{S}$

5. from the $\mathbf{B}$ matrix get $C'_{kn} = \dfrac{(\omega_n^2 - \omega_k^2)B_{kn}}{\omega_n}$ for $k = n = 1, 2 \cdots N; k \neq n$ and $C'(n,n) = 2\Im(\bar{\omega}_n)$

6. from the last steps we have the full $\mathbf{C}'$ matrix. Carry out the transformation $\mathbf{c} = \mathbf{U}^{\mathbf{t}}\mathbf{C}'\mathbf{U}$ to get the damping matrix in physical coordinates

Now it may be observed that even if the transfer functions are symmetric, from the above mentioned procedure there is no definite mathematical reason why the fitted damping matrix will always be symmetric. If we indeed detect a non-symmetric dissipation function then it may be guessed that physical the law behind the damping mechanism in the structure is not viscous. However it seems that by carrying out a method like this it is not possible to guess what is the physical mechanism governing the damping in a structure other than guessing it is non-viscous for a asymmetric fitted dissipation function.

2.5 Example: Axially Vibrating Rod

In this section we have tried to fit a dissipation function model in place of the general damping model for the axially vibrating rod example considered in section 2.2.3. The general method proposed in section 2.4.3 has been used here in order to find out the spatial distribution of damping. The two sets of parameter values used in section 2.2.3 is taken to illustrate different possibilities.

2.5.1 Parameter Set 1:

Damping Model 1:
Figure 2.7 shows the fitted dissipation function $c(x,z)$ for damping model 1. It may be noted that although we have started with a locally reacting damping model, which means the function is non-zero only along $x = z$ straight line, the non-zero values other than $x = z$ line shows that the fitted dissipation function is not locally reacting. The diagonal of this function is shown in figure 2.8. The straight line in this figure corresponds to the position of the general damping function originally present in the structure. From this diagram it is interesting to observe that in-spite-of the spatial distribution of $c(x,z)$ does not match with the spatial distribution of the original distribution the general damping, along the diagonal it matches reasonably well. This in turn means that, an imposed locally reacting assumption on the fitted dissipation function can indicate the location of the general damping present in the structure. For judging the numerical value of the fitted dissipation function we compare the transfer functions calculated from four possible methods. These methods are:

- *Method 1:* By inverting the dynamic stiffness matrix of the form given in equation (2.25) for a system with general damping. Other than involving modal truncation errors this method is exact.

- *Method 2:* By using the expression (2.29) developed earlier for approximate transfer functions for a system with general damping using small damping assumption.
- *Method 3:* By inverting the dynamic stiffness matrix of the form given in equation (2.13) using the fitted dissipation function. Other than involving modal truncation errors this method is exact for the fitted dissipation function.
- *Method 4:* By using the expression (2.19) developed earlier for approximate transfer functions using the fitted dissipation function.

A typical transfer function $H(x, z, \omega)$, for $x = 0.75$ and $z = 1.6$ calculated from the above four methods is shown in figure 2.9. Value obtained form all the four different methods agrees quite well. This indicates that even we didn't obtain very accurate spatial distribution of the fitted dissipation function obtained form this predicts same value as that of the system with general damping model. The results in figure 2.9 have one more far reaching indication, a different damping model (the fitted dissipation function) with a different spatial distribution can give rise to similar transfer function with another damping model having another spatial distribution. This means that by measuring transfer function it is not always possible to find out what is the governing mechanism and moreover it does not matter from the point of view of result. From figure 2.7 it can also be seen that the fitted dissipation function is not symmetric in the original spatial coordinate. It is interesting to check the symmetry property of the transfer functions. Figure 2.10 shows the plot of the transfer functions $H(x, z, \omega)$ and $H(z, x, \omega)$ using method 3 and 4 with the fitted dissipation function. All the calculated transfer functions matches quite well. This plot shows that the non-symmetry of the fitted dissipation function in the spatial coordinate does not effect the symmetry of the transfer functions to the extent it can show significant difference. In this context it would be interesting to observe the effect of symmetry of the fitted dissipation function $c(x, z)$ on detecting the spatial distribution of damping. It is possible to symmetrize the function $c(x, z)$ as, $c(x, z) = \dfrac{c(x, z) + c(z, x)}{2}$, but it has no effect on detecting the spatial distribution of the damping from the diagonal of $c(x, z)$ as can be shown by the (*)-lined plots in the figure 2.8.

Damping Model 2:

Figure 2.11 shows the fitted dissipation function $c(x, z)$ for the damping model 2. As can be seen from the diagram that for this damping model the fitting in spatial domain becomes less accurate compared to the model 1. However, diagonal of the fitted dissipation function shown in figure 2.12 still predicts the spatial distribution reasonably well as it has done for the previous damping model. Transfer function $H(x, z, \omega)$, at $x = 0.75$ and $z = 1.6$ calculated from the four methods described before is shown in figure 2.13. Values obtained form all the four different methods agrees as well as damping model 1, although the spatial distribution of the fitted dissipation function $c(x, z)$ appears to be less accurate. From the plot of transfer functions $H(x, z, \omega)$ and $H(z, x, \omega)$ in figure 2.14 it is also observed that increased asymmetry

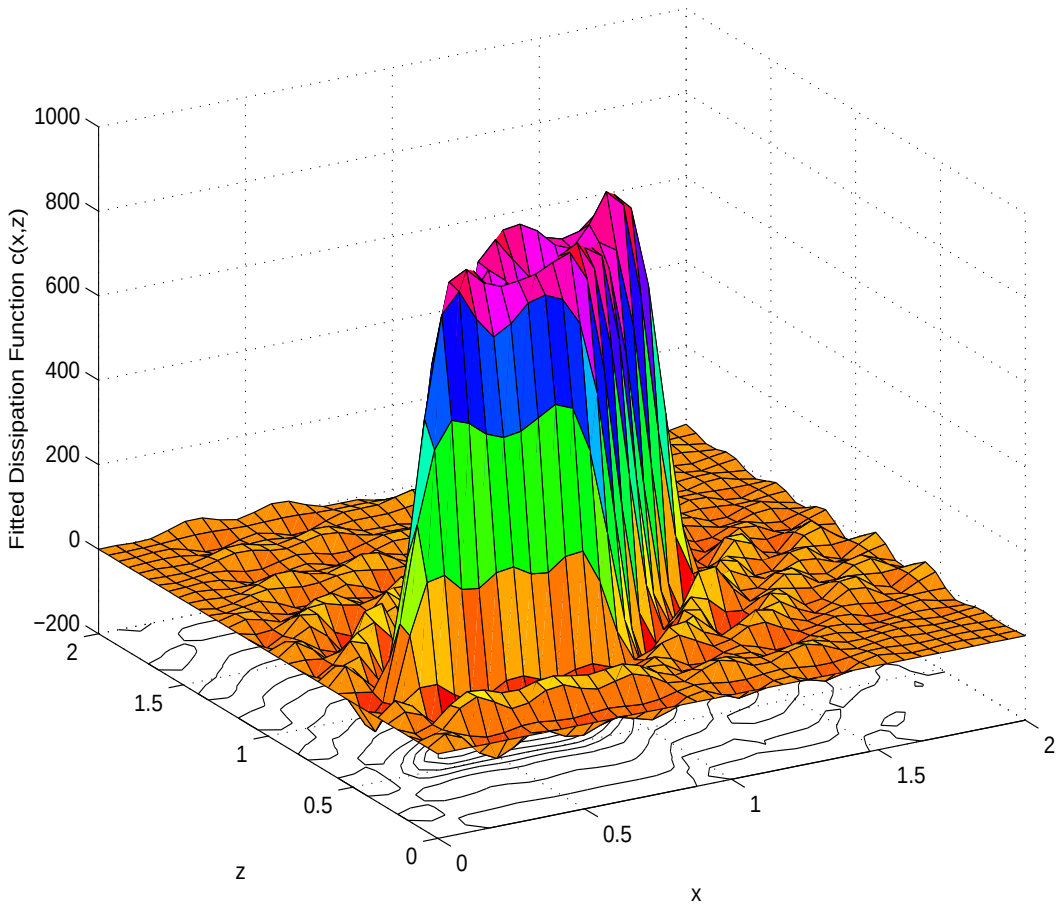

Figure 2.7: Fitted dissipation function $c(x, z)$, damping model 1, parameter set 1

in the fitted dissipation function does not have much effect on preserving symmetry of the transfer functions.

Damping Model 3:
Figure 2.15 shows the fitted dissipation function $c(x, z)$ for the damping model 3. For this damping model, the fitting of the dissipation function in spatial domain is very much similar as for the model 1. Diagonal of the fitted dissipation function shown in figure 2.16 still predicts the spatial distribution reasonably well as it was for the previous two damping models. Transfer function $H(x, z, \omega)$, at $x = 0.75$ and $z = 1.6$ calculated from the four methods described before is shown in figure 2.17. Like previous two damping models the values obtained form all the four different methods agrees well. From the plot of transfer functions $H(x, z, \omega)$ and $H(z, x, \omega)$ in figure 2.18 it can be observed that the for this damping model also symmetry property of the transfer functions remains preserved.

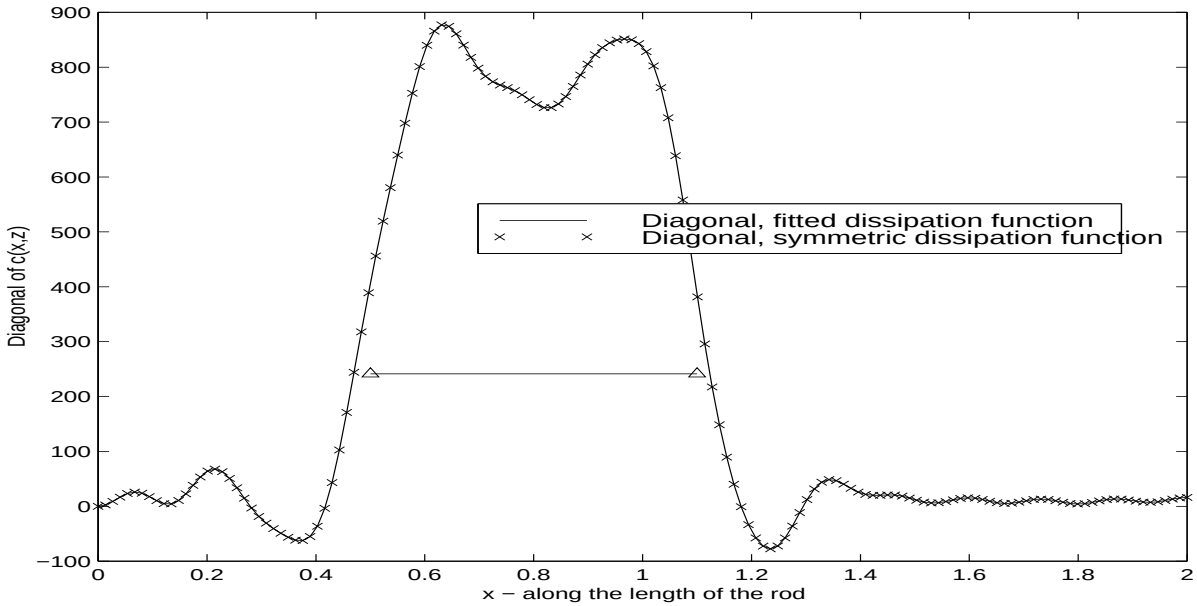

Figure 2.8: Diagonal of the fitted dissipation function $c(x, z)$, damping model 1, parameter set 1

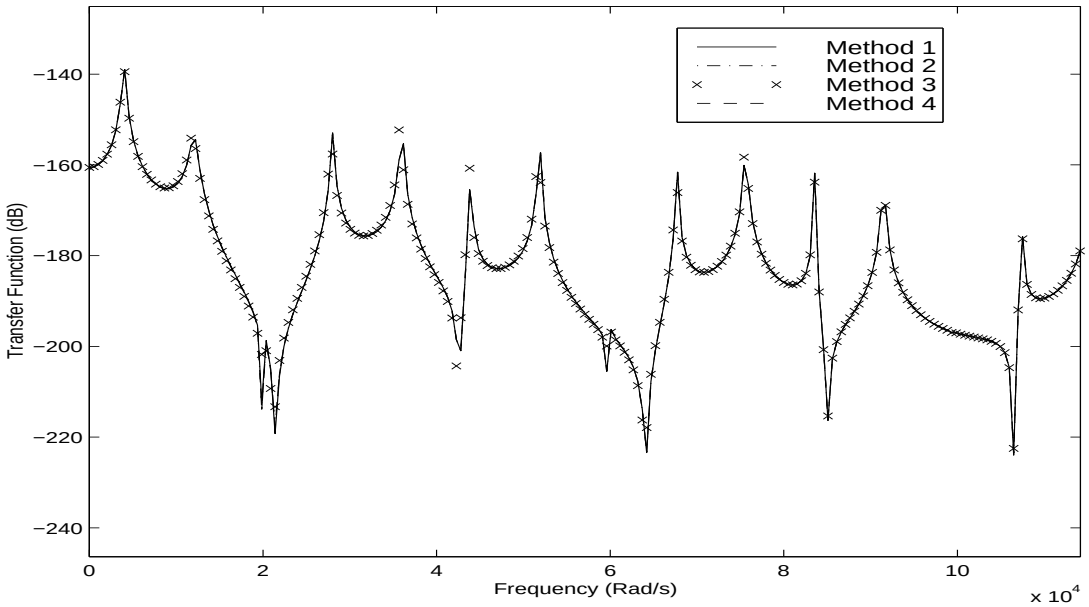

Figure 2.9: Transfer function $H(x, z, \omega)$, $x = 0.75$, $z = 1.6$, damping model 1, parameter set 1

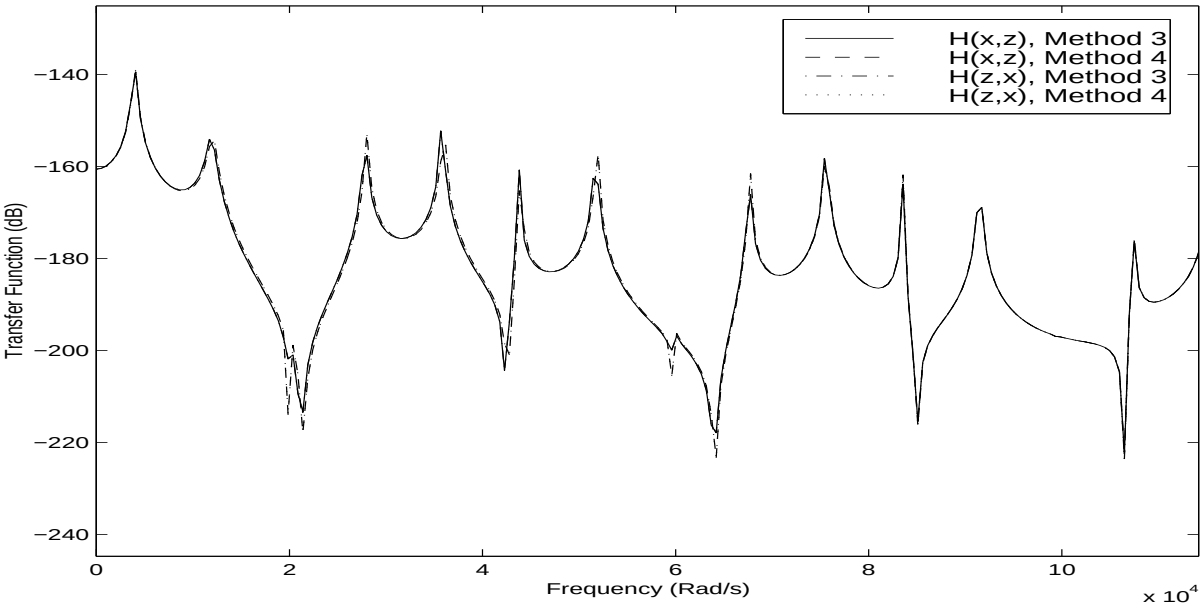

Figure 2.10: Transfer function $H(x, z, \omega)$ and $H(z, x, \omega)$, $x = 0.75$, $z = 1.6$, damping model 1, parameter set 1

So, as a summary, for all the three damping models with parameter set 1 it can be said that with the fitted dissipation function model, the predicted transfer functions matches quite well with the original transfer functions. By and large, all the models show non-locally reacting and asymmetric spatial distribution of the fitted dissipation function model while model 2 becomes more non-locally reacting than the other two models. Inspite of asymmetric spatial distribution of the fitted dissipation function, the transfer functions remains symmetric. How much non-locally reacting or assymetric be the spatial distribution of the fitted dissipation function $c(x, z)$ in xz-plane, the diagonal of $c(x, z)$ seems to be robust in locating the spatial distribution of the locally reacting general damping in the structure.

2.5.2 Parameter Set 2:

Damping Model 1:
With parameter set 2, figure 2.19 shows the fitted dissipation function $c(x, z)$ for damping model 1. Unlike parameter set 1, here the locally reacting nature of the assumed damping model is more well represented by the fitted dissipation function. The diagonal of this function is shown in figure 2.20. As expected, the diagonal of $c(x, z)$ predicts the position of the general damping function originally present in the structure quite well. The transfer function $H(x, z, \omega)$, for the same locations, $x = 0.75$ and $z = 1.6$ calculated from the four methods described earlier is shown in figure 2.9. Values obtained form all the four different methods agrees quite well. The reciprocity of the transfer functions has also been checked (not shown

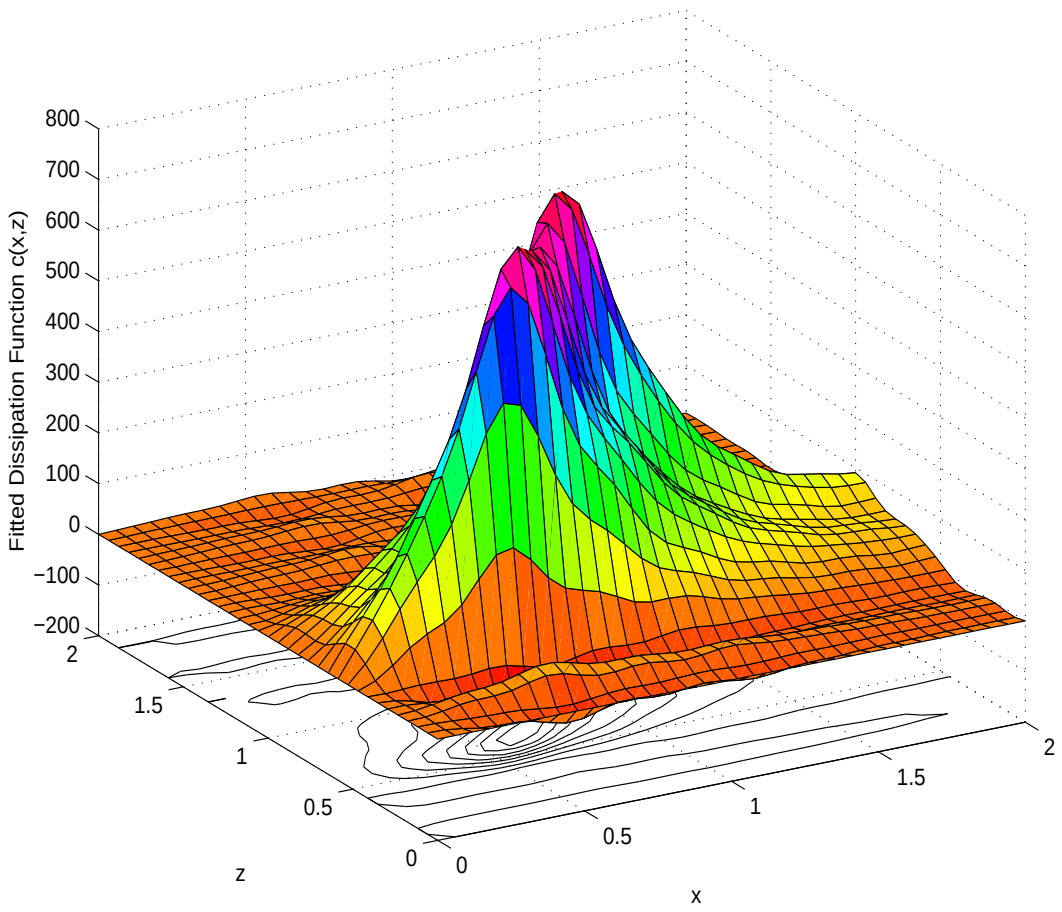

Figure 2.11: Fitted dissipation function $c(x, z)$, damping model 2, parameter set 1

in a figure) and observed to be alright.

Figure 2.22 and 2.24 shows the fitted dissipation function $c(x, z)$ for the damping model 2 and 3 respectively. The transfer functions at the previous locations for damping model 2 and 3 are shown in figures 2.23 and 2.25 respectively. It can be observed that all the properties that has been discussed so far, for these two damping models remains very much similar to that of the model 1.

So, in summary, it can be said that for parameter set 2, all the three damping models behaves very much in a similar way. With the fitted dissipation function model, the predicted transfer functions matches quite well with the original transfer functions. From table 2.1 It may be noted that the Q-factors for parameter set 2 is quite low but still we get a good agreement of the transfer functions calculated by all the four methods described earlier. Unlike for parameter set 1, all the models show locally reacting and symmetric spatial distribution of the fitted dissipation function model $c(x, z)$. Like parameter set 1, the diagonal of $c(x, z)$ locates the spatial distribution of the locally reacting general damping in the structure quite

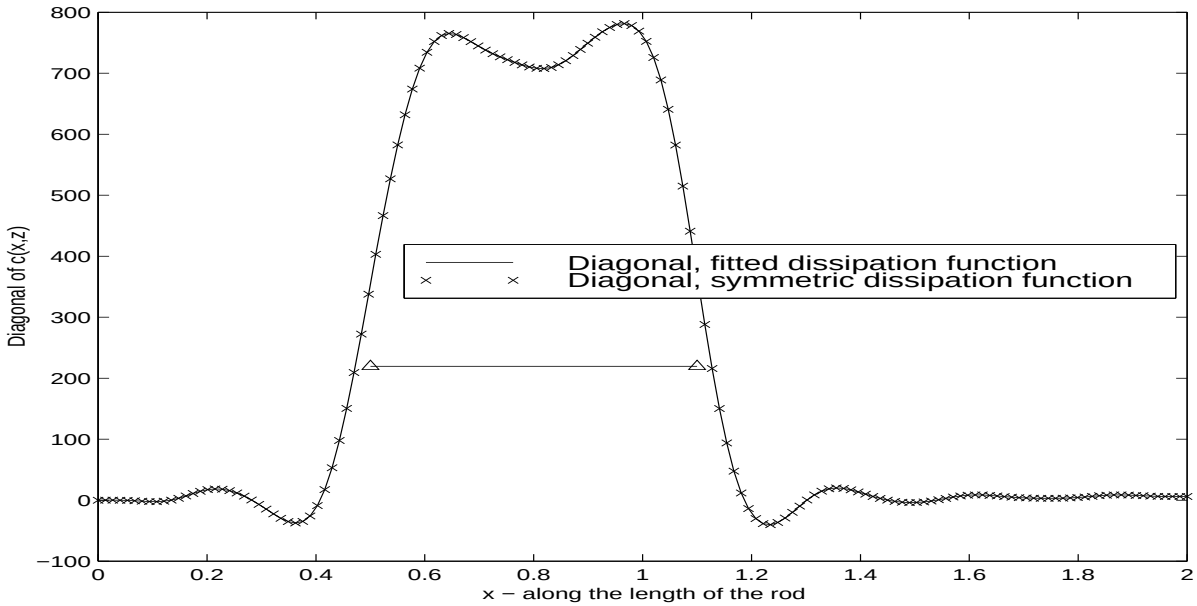

Figure 2.12: Diagonal of the fitted dissipation function $c(x, z)$, damping model 2, parameter set 1

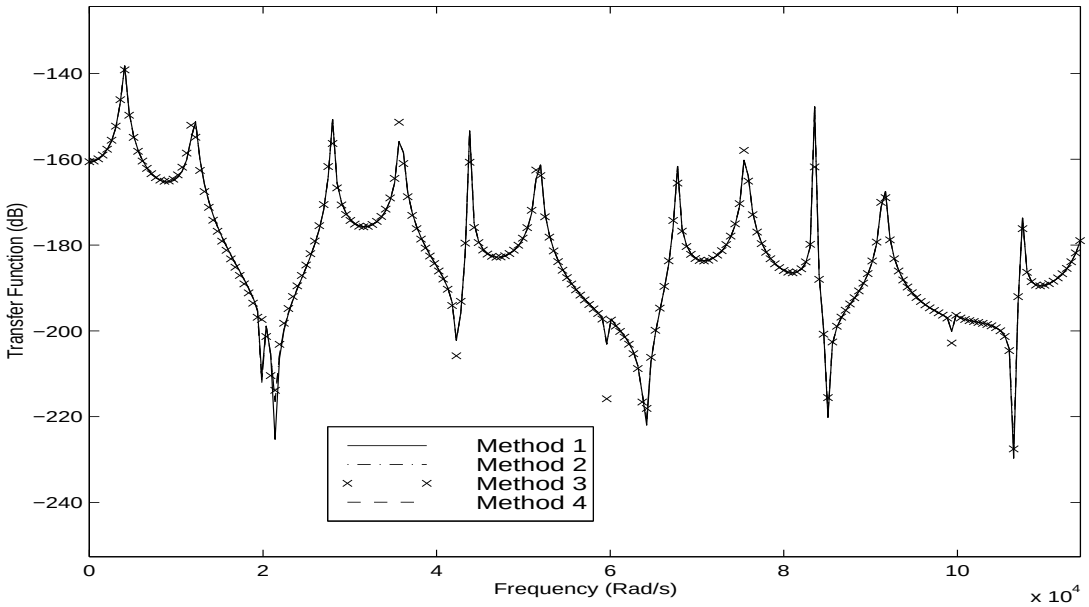

Figure 2.13: Transfer function $H(x, z, \omega)$, $x = 0.75$, $z = 1.6$, damping model 2, parameter set 1

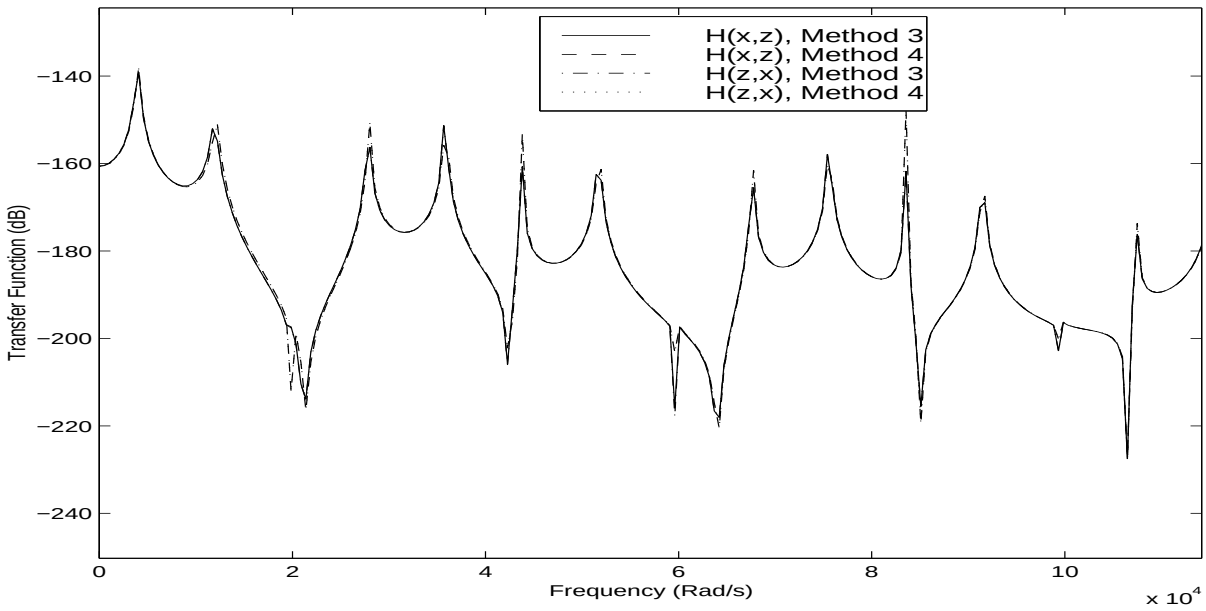

Figure 2.14: Transfer function $H(x, z, \omega)$ and $H(z, x, \omega)$, $x = 0.75$, $z = 1.6$, damping model 2, parameter set 1

well.

2.5.3 Discussion

We have done few more numerical experiments with different sets of parameter values but it was observed that the essential features of the results remain more or less the same and can effectively be represented by the two parameter sets considered here. Based on our study, few general observation can be made. Whatever the values of the Q-factors or nature of the the fitted dissipation function $c(x, z)$ in xz-plane be, the transfer function obtained form the fitted dissipation function agrees well with the transfer of the system with the assumed locally reacting general damping models. The symmetric property of the transfer function remains preserved within an acceptable accuracy although in some cases the fitted dissipation function $c(x, z)$ is not exactly symmetric in spatial coordinate. Looking at the diagonal of $c(x, z)$ appears to be a robust technique for detecting the spatial distribution of the locally-reacting general damping model originally assumed for the structure.

It is of interest to us to investigate and understand the implication of symmetry breaking of the fitted dissipation function $c(x, z)$ in xz-plane. For parameter set 1 the area under the damping functions $g_t(t)$ remains same with parameter set 2 and Q-factors are higher than parameter set 2. However, It was shown before that preserving the area under $g_t(t)$ or the Q-factors does not have much affect of the result. The difference occurs due to the difference in the values of the constants t_1 , λ and t_3 defined in equations (2.33 $\cdots$ 2.35). In fact

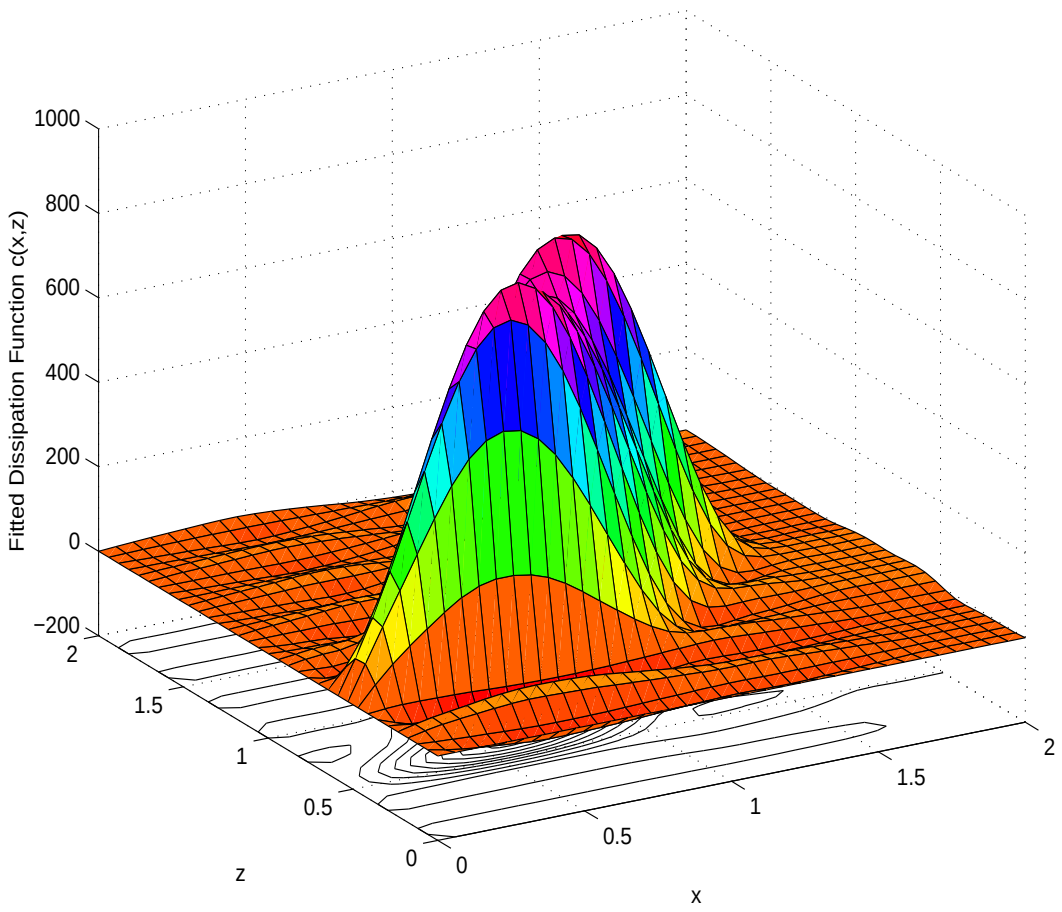

Figure 2.15: Fitted dissipation function $c(x, z)$, damping model 3, parameter set 1

for parameter set 1, t_1 and t_3 become larger and λ becomes smaller compared with that of parameter set 2. This in turn means that for parameter set 1 the damping function in time domain have a large memory, or in terms of frequency domain, have more rapidly varying spectrum compared to parameter set 2. So, more the damping functions are away form the delta function (*i.e.* away form viscous damping) the more becomes the asymmetry and non-locally-reactingness in the fitted dissipation function. This behaviour however is expected. So in conclusion it can be said that it is the memory of the damping functions that effects more the fitting procedure than the Q-factors or any other factors. In case we detect a asymmetric non-locally reacting equivalent dissipation function model, we can say that the nature of the damping mechanism present in the structure in not viscous. However, from the study conducted so far, if the original damping mechanism in the structure is not viscous then what mechanism it could possibly be can not be guessed. At last, it may be observed that, the actual mechanism that governs the damping in a structure does not really matter from an engineering point of view, since for any damping mechanism an equivalent dissipation

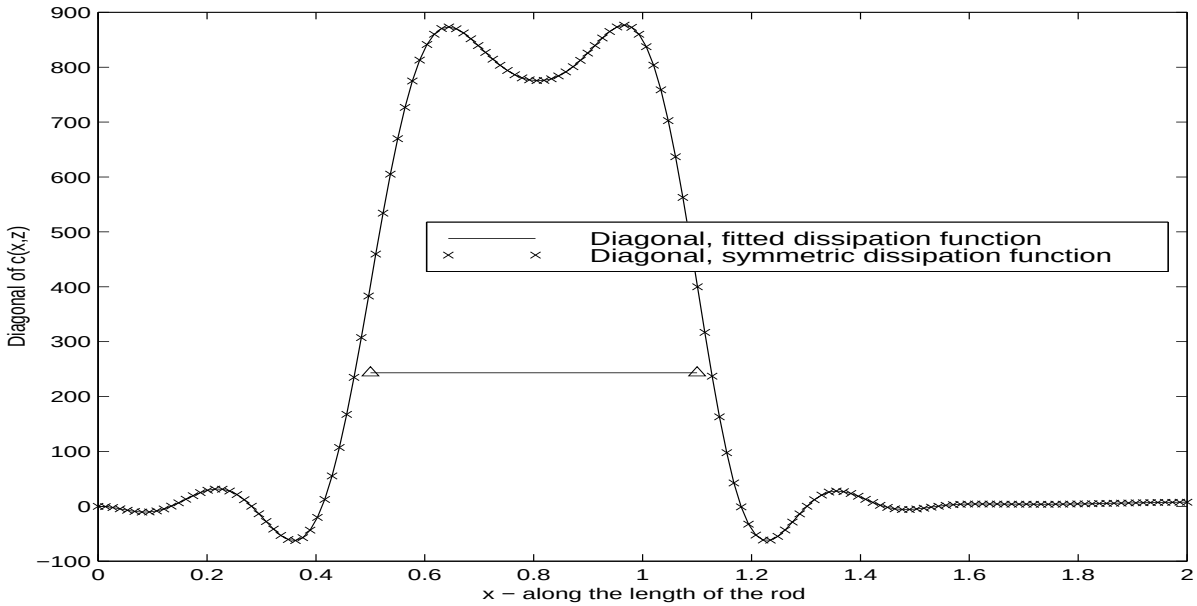

Figure 2.16: Diagonal of the fitted dissipation function $c(x, z)$, damping model 3, parameter set 1

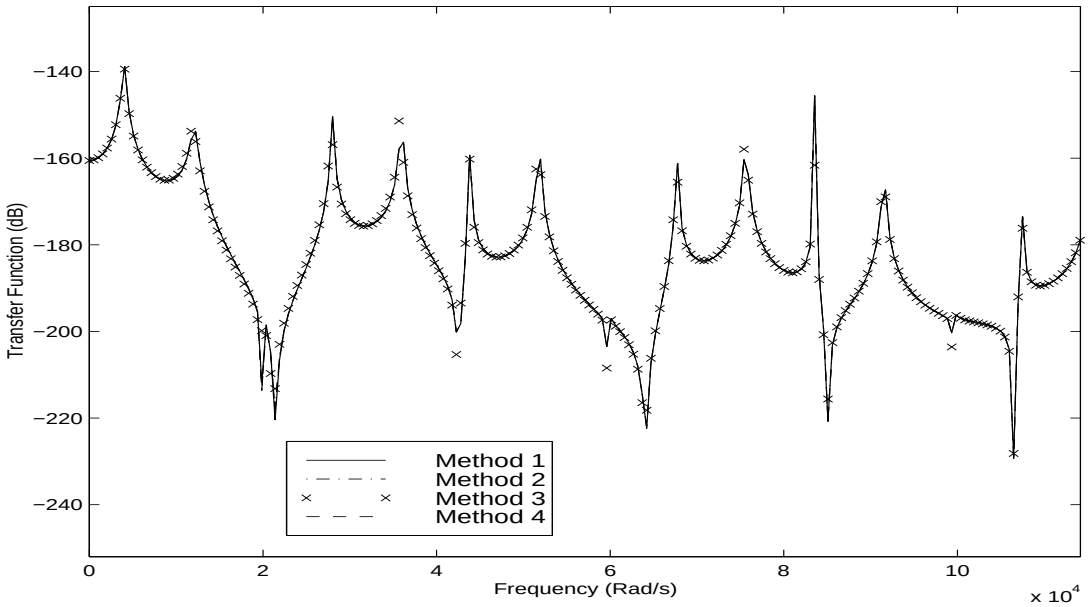

Figure 2.17: Transfer function $H(x, z, \omega)$, $x = 0.75$, $z = 1.6$, damping model 3, parameter set 1

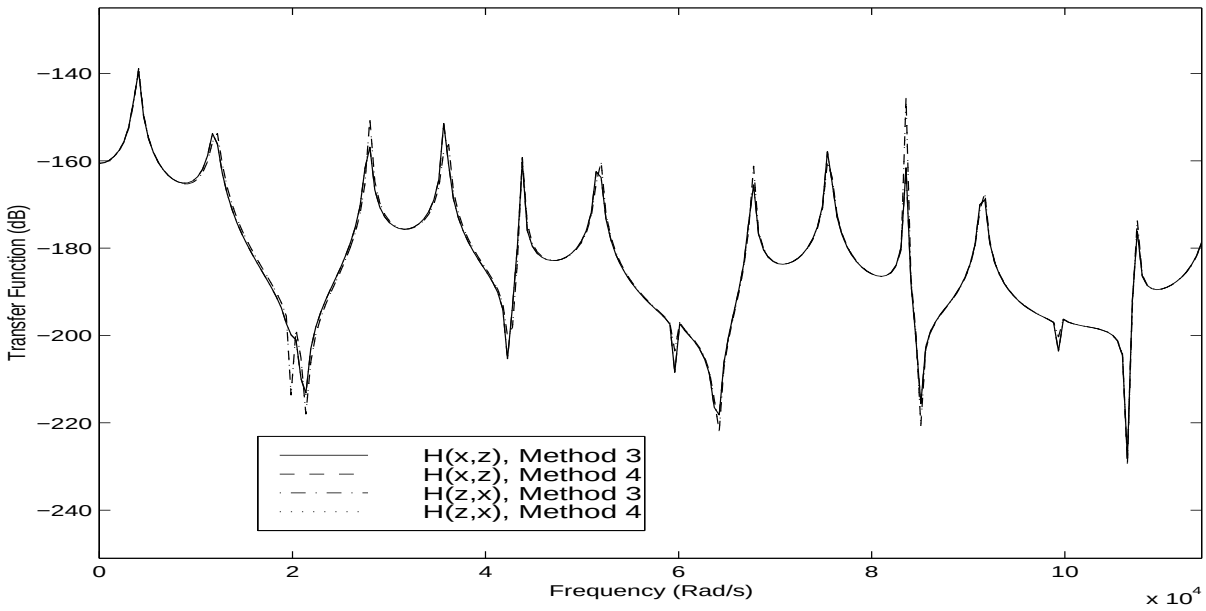

Figure 2.18: Transfer function $H(x, z, \omega)$ and $H(z, x, \omega)$, $x = 0.75$, $z = 1.6$, damping model 3, parameter set 1

function can be fitted and used for later calculations.

2.6 Example: N Spring-Mass Systems

An linear array of N spring-mass oscillator has been considered in this section and is shown in Figure 2.26. The mass of each block is m and coupling stiffness between them is taken as k. This example is aimed at simulating the axially vibrating rod considered in the last section in a discrete sense. It can be shown that by choosing $m = \frac{1}{N}\rho L$ and $k = \frac{AE}{L}N$, this system can very closely represent the axially vibrating rod as N approaches to a large value. In order to justify the locally-reacting assumption in the axially vibrating rod example studied before, it is also considered that damping associated with each mass is connected with the ground only. Like section 2.2.3, the damping model associated with rth mass is assumed of the form of

$$g_r(t) = g_{(r)} g_t(t) \tag{2.56}$$

In the similar line with the rod example, we take $g_{(r)}$ to be the same for all the damped blocks to represent a 'uniformly distributed damper'. The value of $g_{(r)}$ is obtained as follows: let us consider among the N masses, damping is associated with only between the s-th and $(s + l)$-th masses. In this example we have considered the three models of $g_t(t)$ that has been described before (see equations 2.33 $\cdots$ 2.35) and thus by selecting any such model a

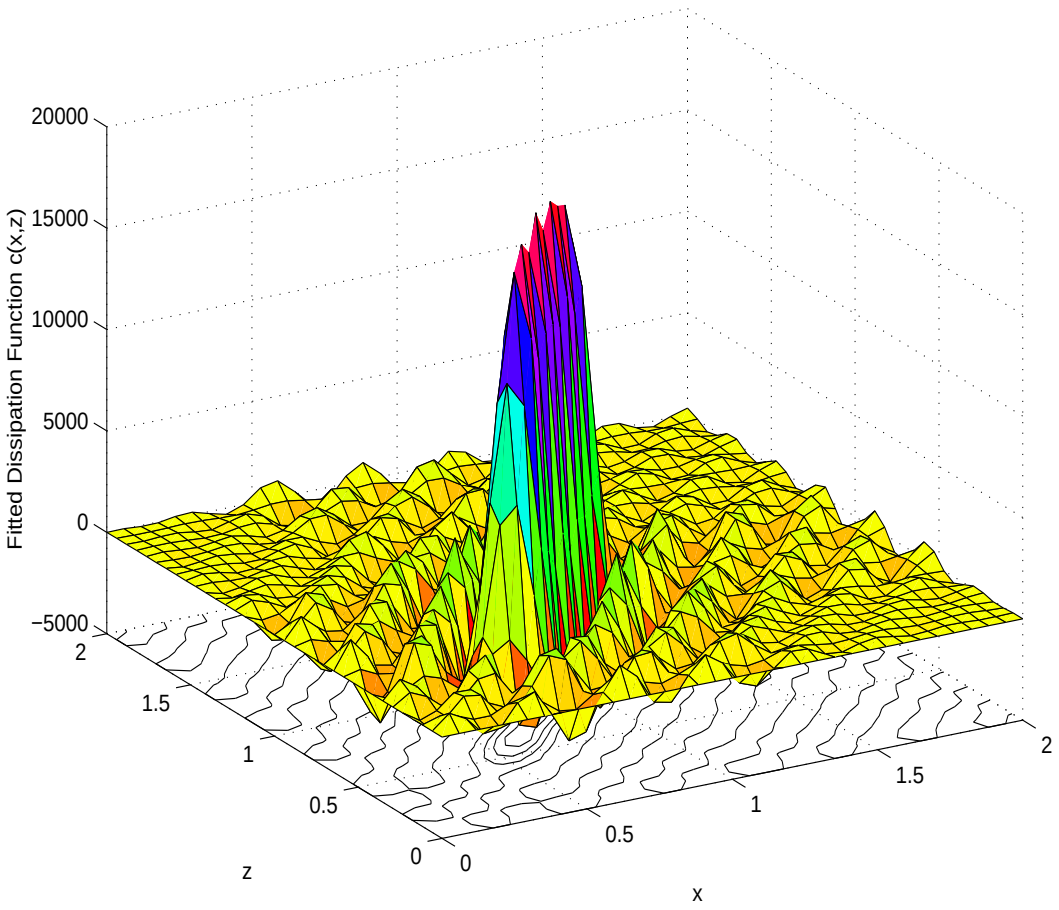

Figure 2.19: Fitted dissipation function $c(x, z)$, damping model 1, parameter set 2

damping anequivalence can be acheived by taking

$$g_{(r)} = g_x \frac{(x_2 - x_1)}{l}.$$

The locations s and $(s + l)$ are selected in such a way that along the length of the linear chain they should roughly correspond to the damped portion of the rod. For the numerical calculation here, we have taken $N = 30$, $s = 8$ and $(s + l) = 17$ and in correspondence with rod example ($x = 0.75$, $z = 1.6$) transfer functions $H(i, j, \omega)$ are calculated at $i = 11$ and $j = 24$ th DOF.

It should be noted that we have conducted extensive numerical investigation for this problem. This study also shows similar behaviour that have been observed in the previous study with some minor difference. However, a limited number of results have been included to support this observation.

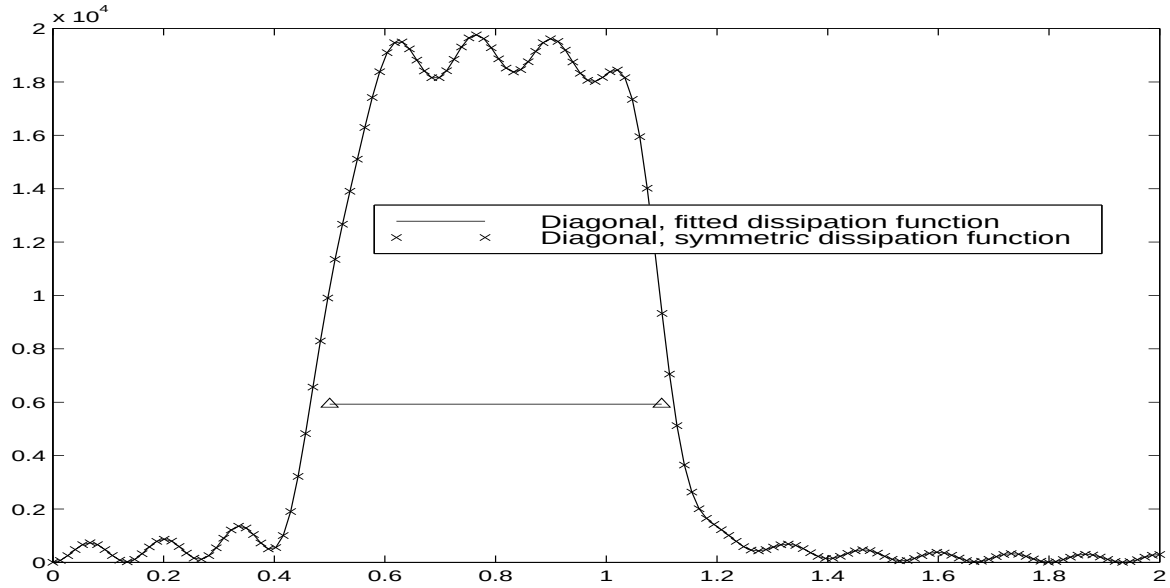

Figure 2.20: Diagonal of the fitted dissipation function $c(x, z)$, damping model 1, parameter set 2

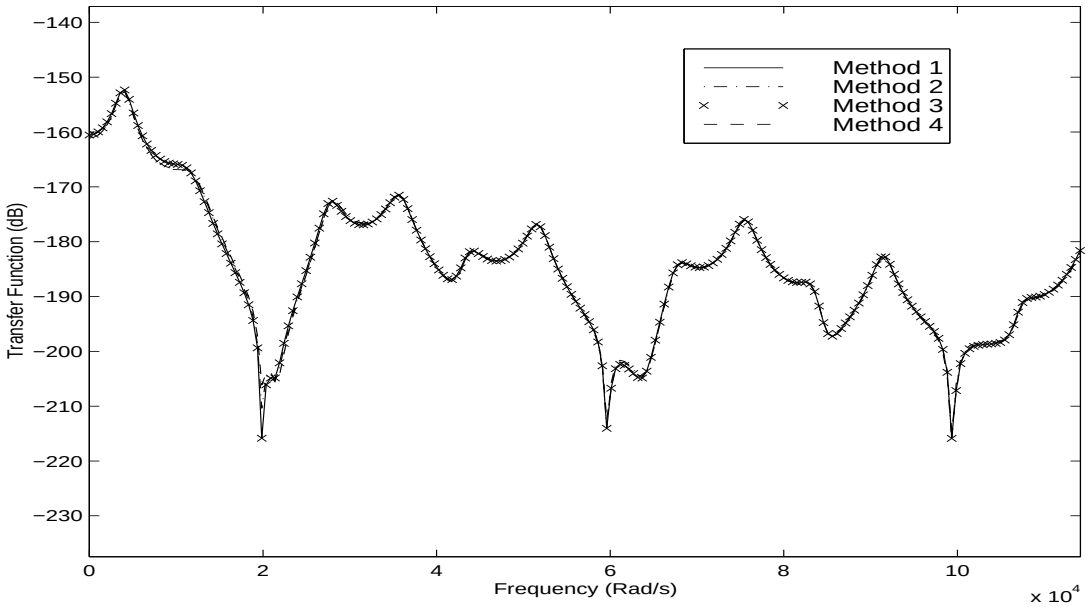

Figure 2.21: Transfer function $H(x, z, \omega)$, $x = 0.75$, $z = 1.6$, damping model 1, parameter set 2

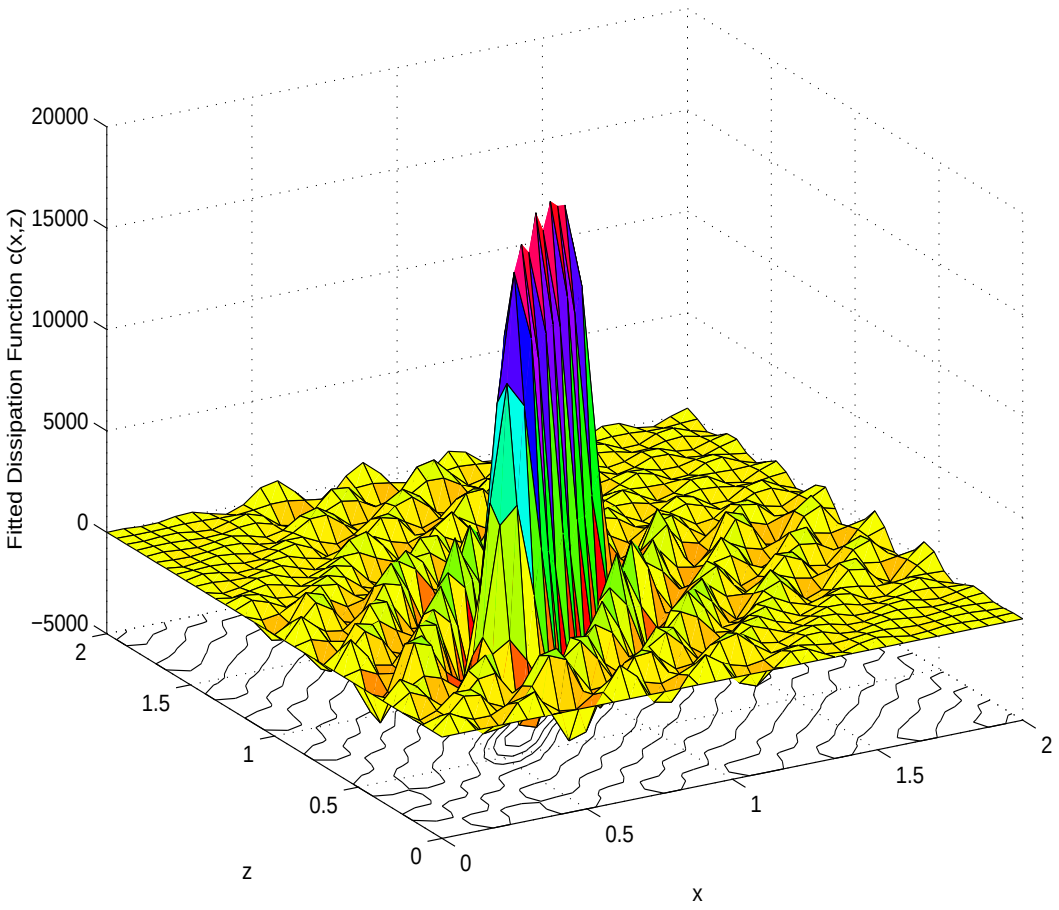

Figure 2.22: Fitted dissipation function $c(x, z)$, damping model 2, parameter set 2

Figures 2.27 $\cdots$ 2.29 shows the fitted dissipation matrix c_{ij} for all the three damping models with parameter set 1. It is interesting to observe that the fitted dissipation matrix c_{ij} become non-locally reacting and the way they are different is very much similar to the corresponding case of the rod example. An apparent difference one might observe that the due to discrete nature of the problem these plots looks more sharp in nature. Fitted dissipation matrix c_{ij} for damping model 2 shows maximum departure from the locally reacting assumption. However, as before, the diagonal of c_{ij} shown in figure 2.30 still predicts the spatial distribution of the damping reasonably well. Transfer function $H_{ij}(\omega)$ for all the damping models, calculated at $i = 11$ and $j = 24$ th DOF from the four methods described before is shown in figures 2.31 $\cdots$ 2.33. Here, with a difference with the axially vibrating rod case, the transfer function obtained by method 2 produces different result. For parameter set 2, we choose to show the results for only damping model 2 since for this model, the fitted dissipation matrix has produced maximum departure from the locally reacting assumption and would be of interest to observe if tend to more locally reacting as it has happened for

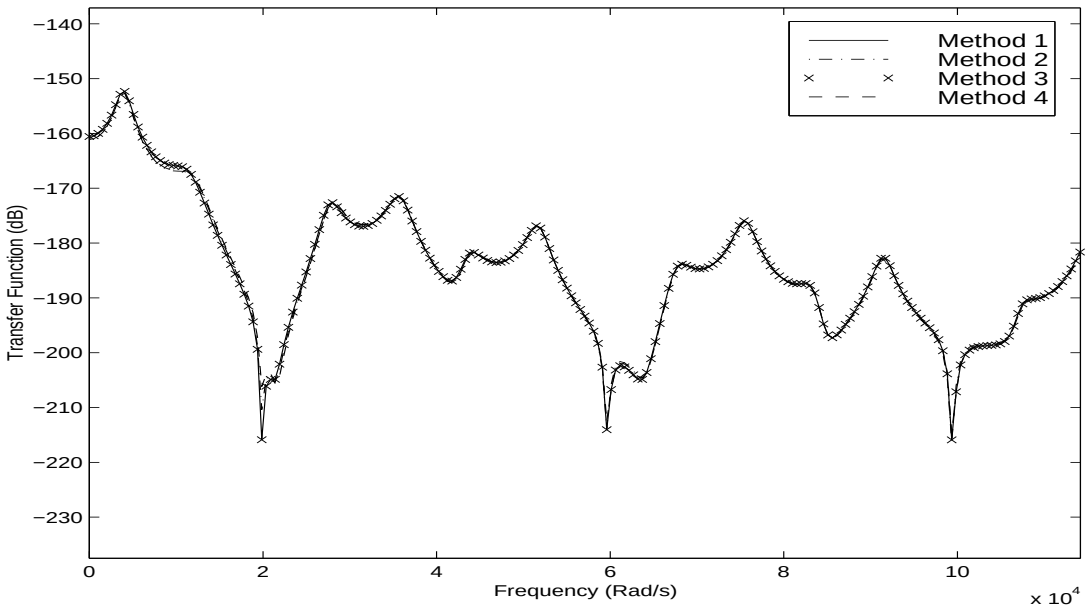

Figure 2.23: Transfer function $H(x, z, \omega)$, $x = 0.75$, $z = 1.6$, damping model 2, parameter set 2

the rod example. Figure 2.34 shows the fitted dissipation matrix for this case and we indeed observe the expected result. This plot also clearly shows the location of the damping in the linear chain system considered. Plot of the transfer function is shown in figure 2.35. Like parameter set 1, other than model 2 prediction from all other 3 methods agrees quite well.

2.7 Conclusions

In this chapter the conventional modal analysis method for linear continuous system is extended to handle general locally reacting damping models. On the account of non-proportional nature of the damping the natural frequencies and mode shapes become complex. Based on the small damping assumption, simple expressions of the natural frequencies and mode shapes has been obtained in terms of undamped system natural frequencies and mode shapes. Like proportionally damped system, an expression of the continuous transfer function is derived in terms of a summation over the complex modes. The developed expressions are exemplified by considering a problem of an axially vibrating rod with damping over a part of its length. Three equivalent but different damping models has been used for the purpose of illustrating different numerical results.

In conjunction to the above formulation of complex natural frequencies and mode shapes, a method has been proposed to detect the spatial distribution of damping in vibrating

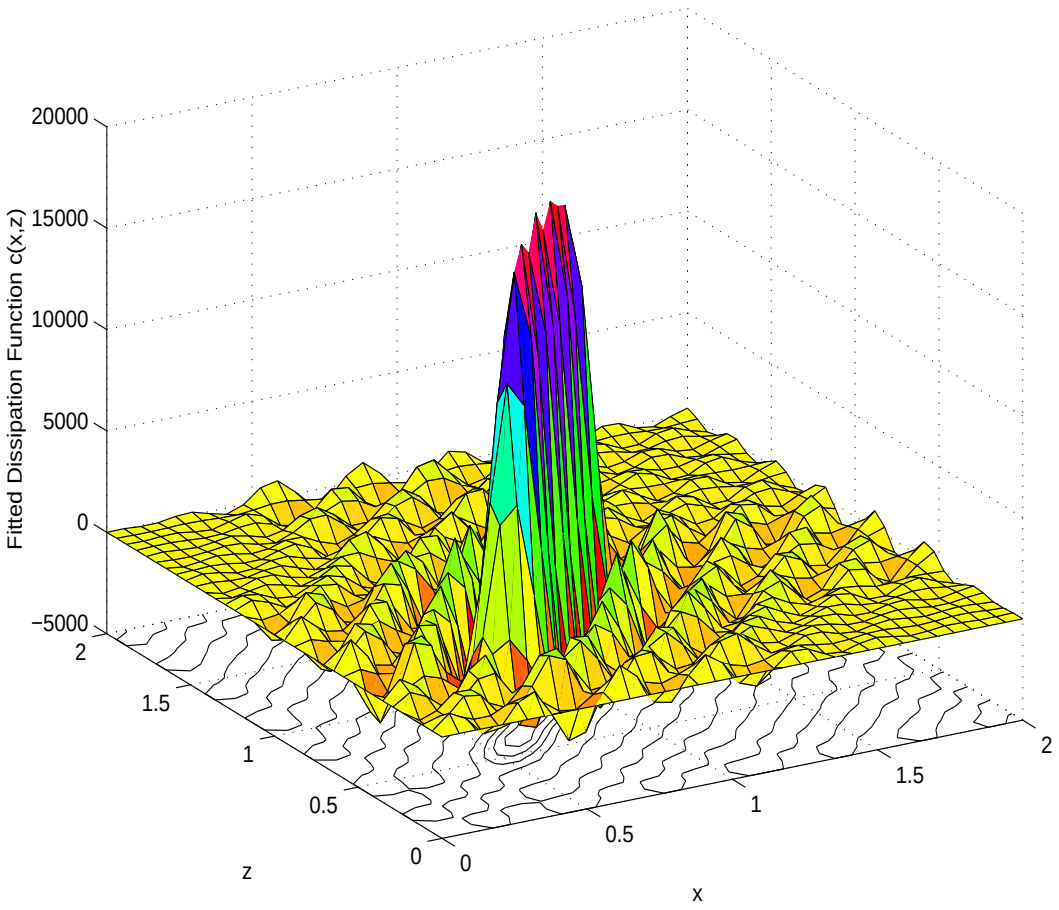

Figure 2.24: Fitted dissipation function $c(x, z)$, damping model 3, parameter set 2

structures. The method is fairly straight forward and easily amenable to the conventional modal testing procedures. Information of the complex modes and natural frequencies appears to be sufficient to carry out the proposed method. Validity of the proposed method is verified by applying it to two commonly occurred problems in structural dynamics: an axially vibrating rod and an N spring-mass oscillator. For most of the test cases considered the developed method predicts the location of the damping with sufficient accuracy. For the cases when the method fails to work or may lead to inaccurate results has been pointed out and intuitive notion has been given for any such disagreement.

With this, the research work taken for this report comes to an end. Based on this work and the literature review conducted in the previous chapter, we have framed a *research proposal* for the future of this ongoing project and is reported in the next chapter.

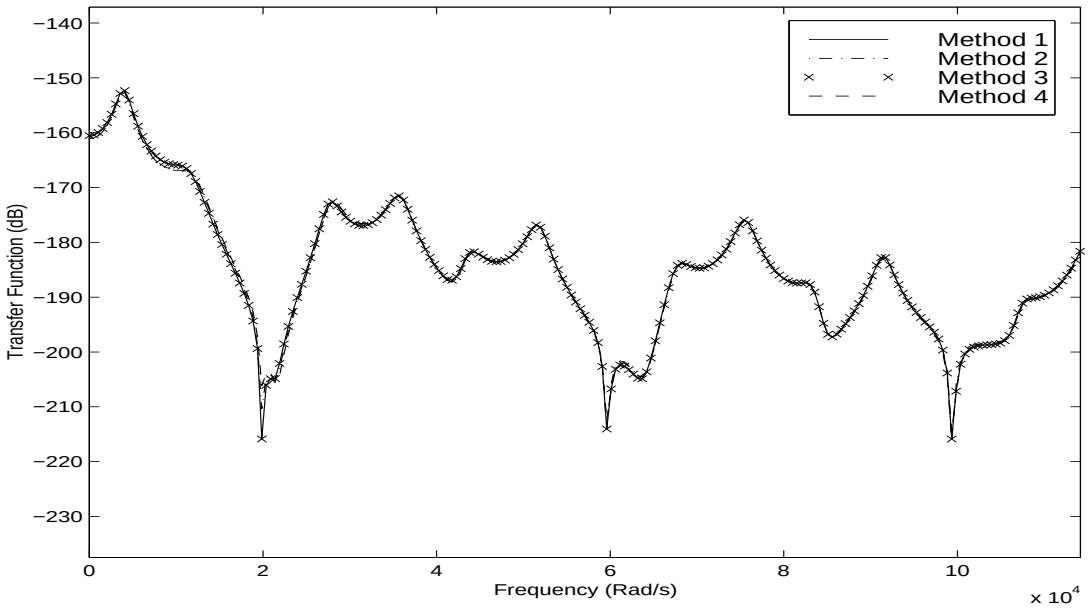

Figure 2.25: Transfer function $H(x, z, \omega)$, $x = 0.75$, $z = 1.6$, damping model 3, parameter set 1

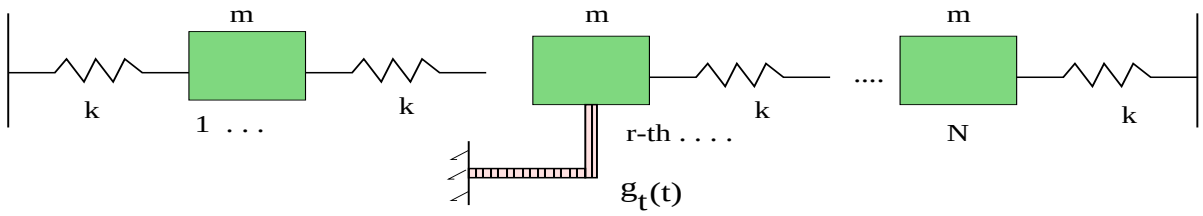

Figure 2.26: Linear array of N spring-mass oscillator, $N = 30$, $m = 0.208\,Kg$, $k = 1.2000 \times 10^9 N/m$

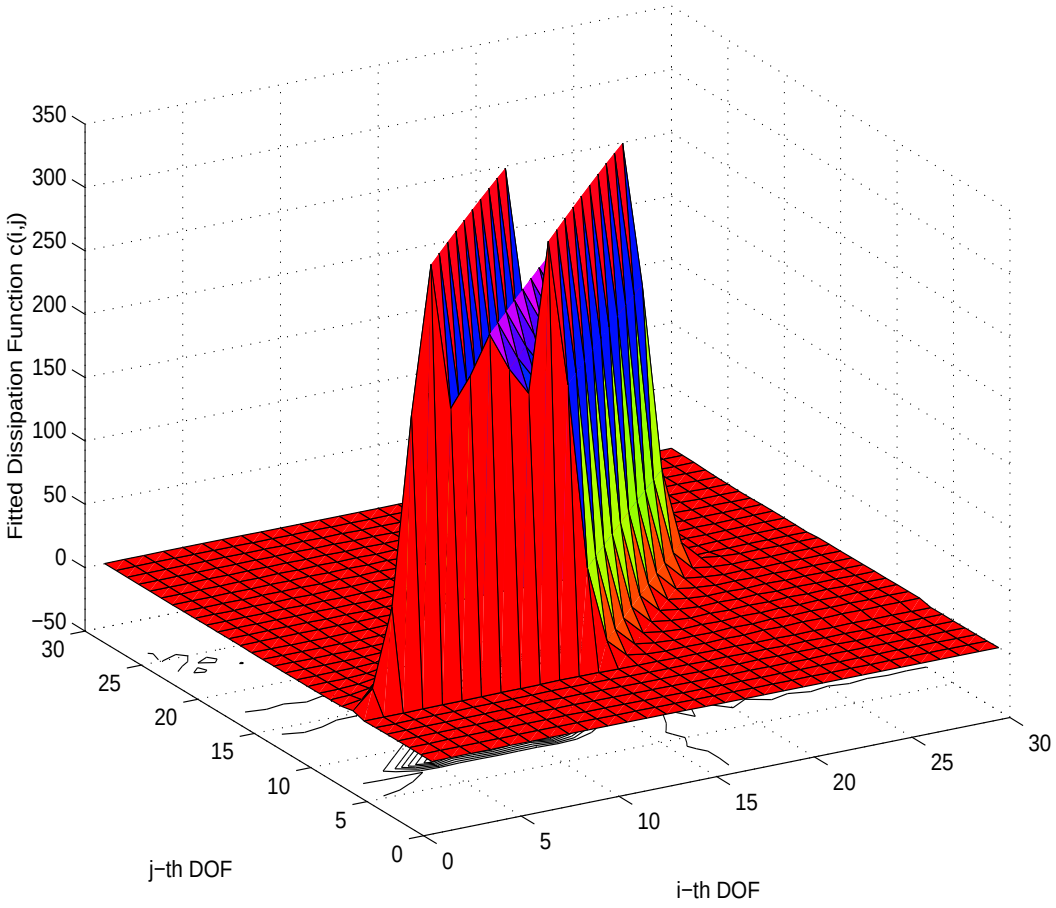

Figure 2.27: Fitted dissipation matrix c_{ij}, damping model 1, parameter set 1

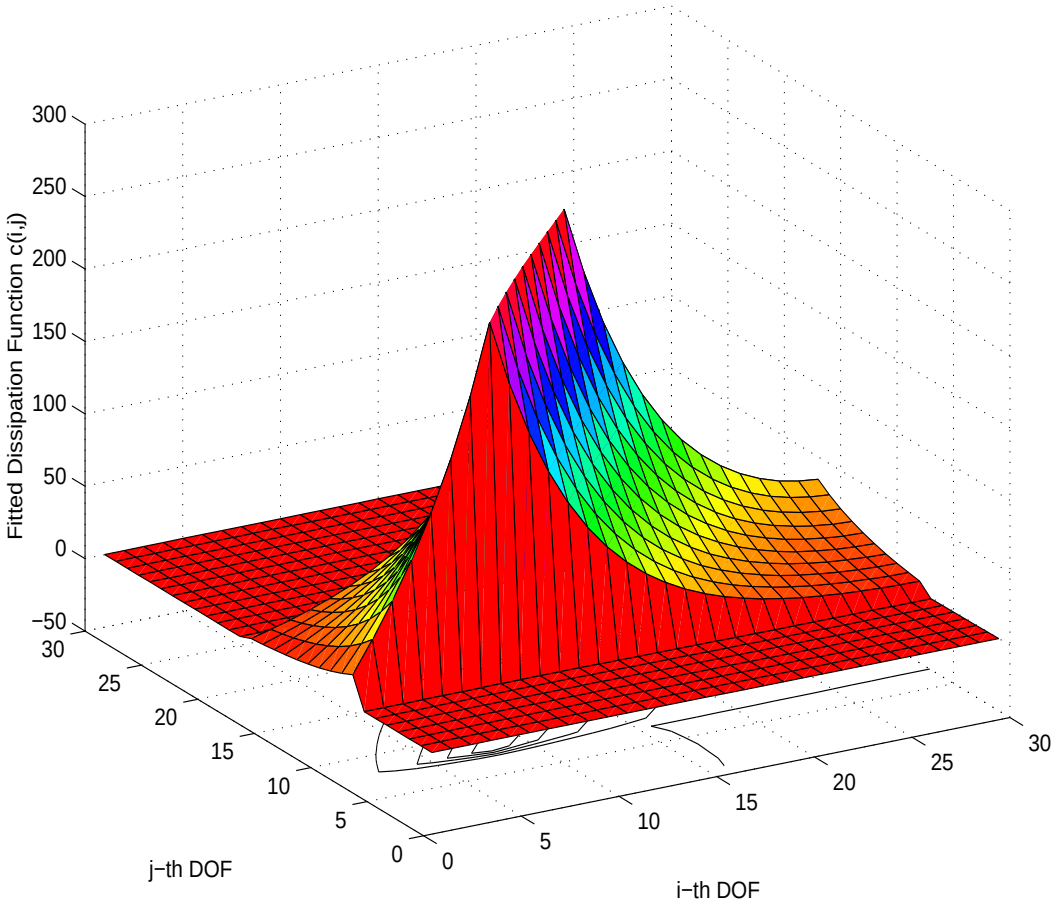

Figure 2.28: Fitted dissipation matrix c_{ij}, damping model 2, parameter set 1

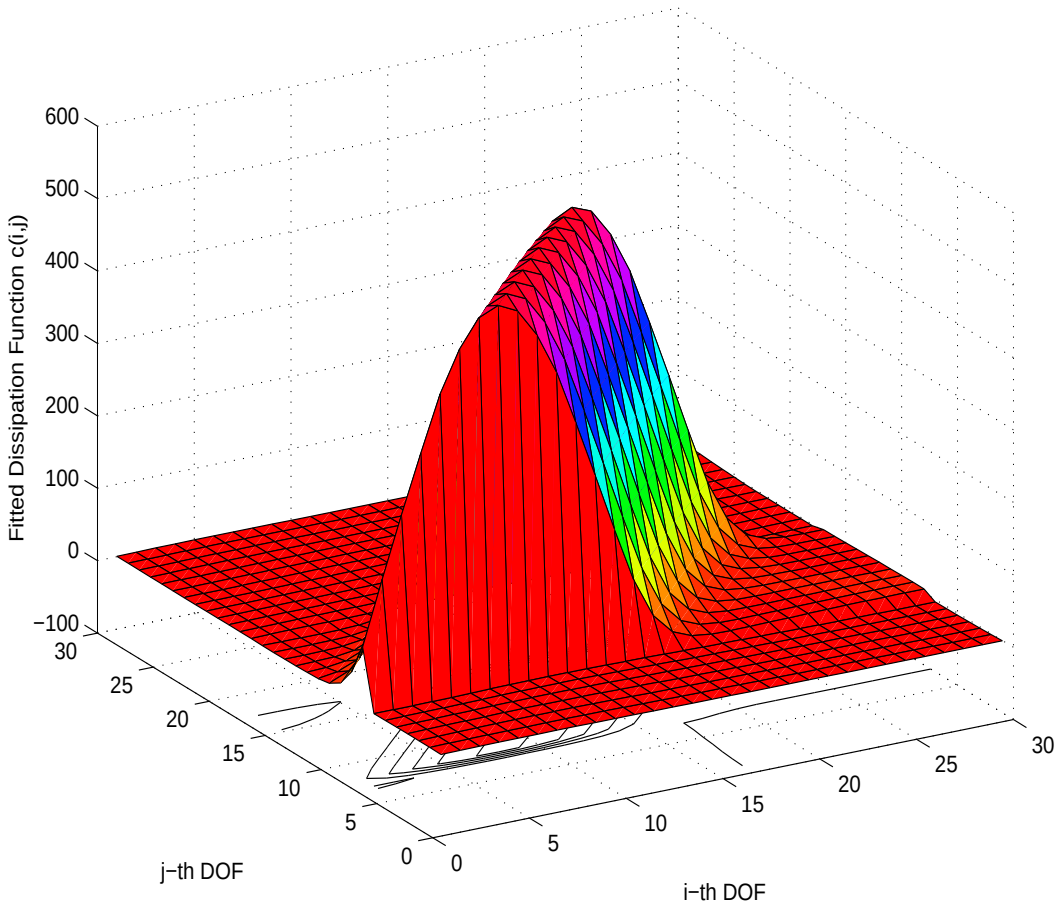

Figure 2.29: Fitted dissipation matrix c_{ij}, damping model 3, parameter set 1

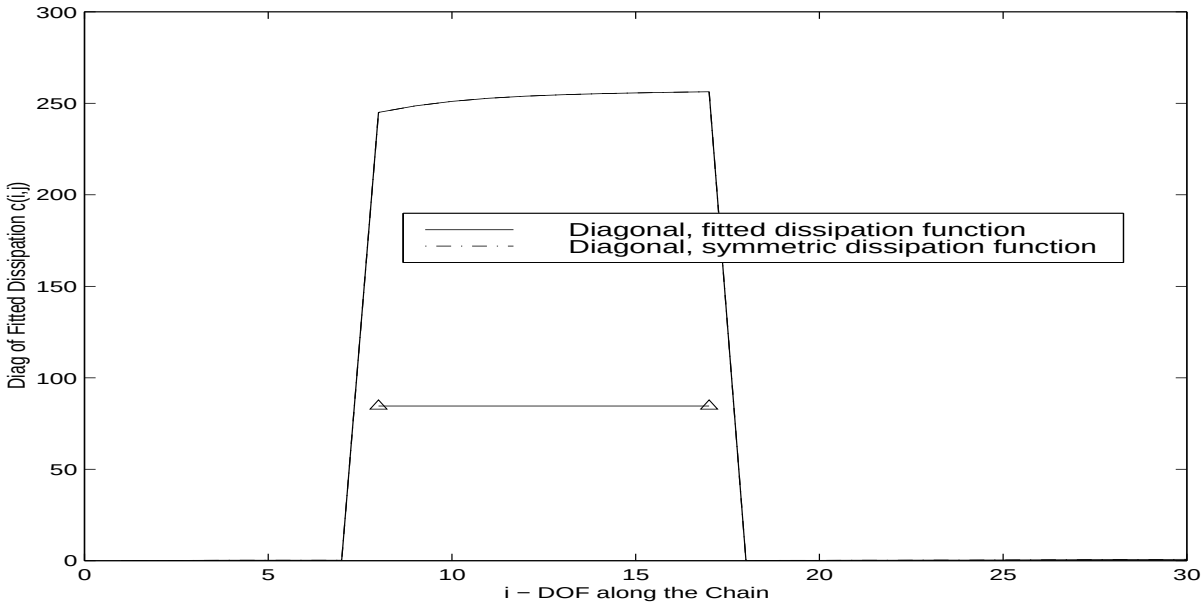

Figure 2.30: Diagonal of the fitted dissipation matrix c_{ij}, damping model 2, parameter set 1

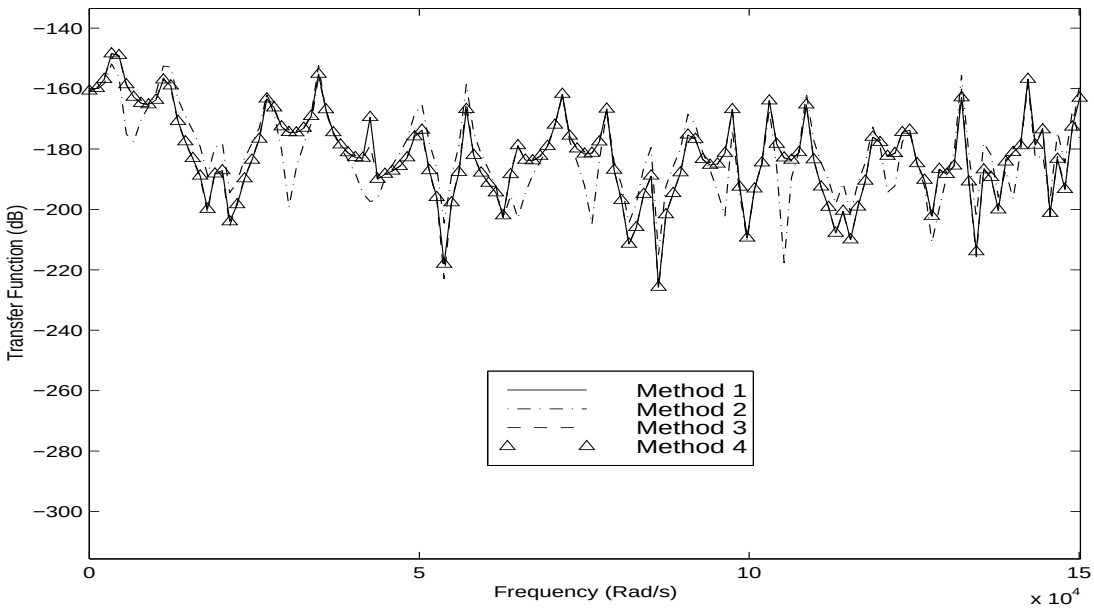

Figure 2.31: Transfer function $H_{ij}(\omega)$, $i = 11$ and $j = 24$, damping model 1, parameter set 1

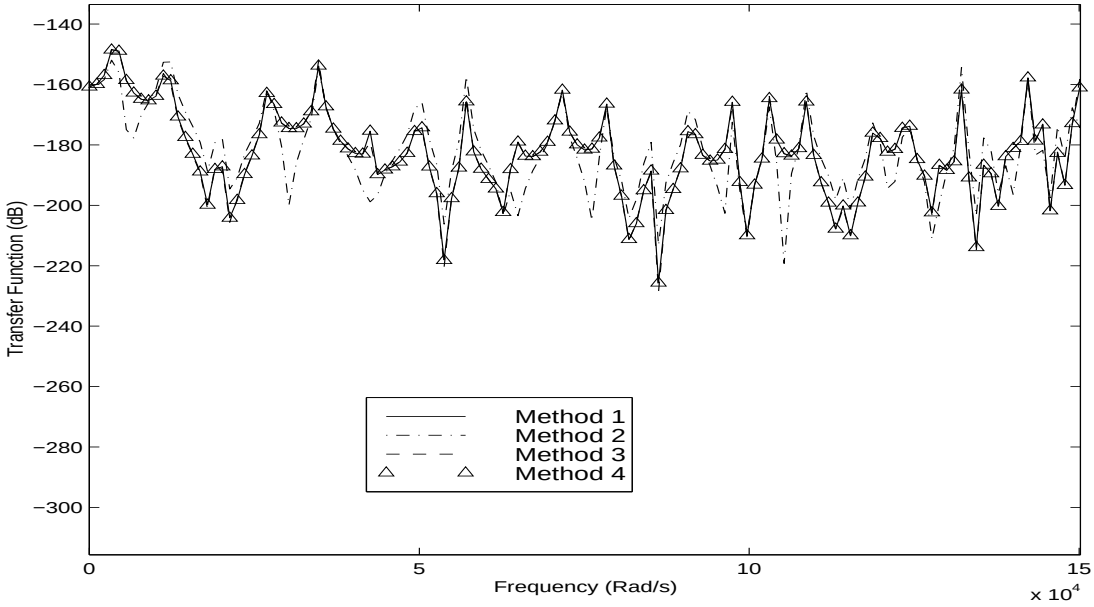

Figure 2.32: Transfer function $H_{ij}(\omega)$, $i = 11$ and $j = 24$, damping model 2, parameter set 1

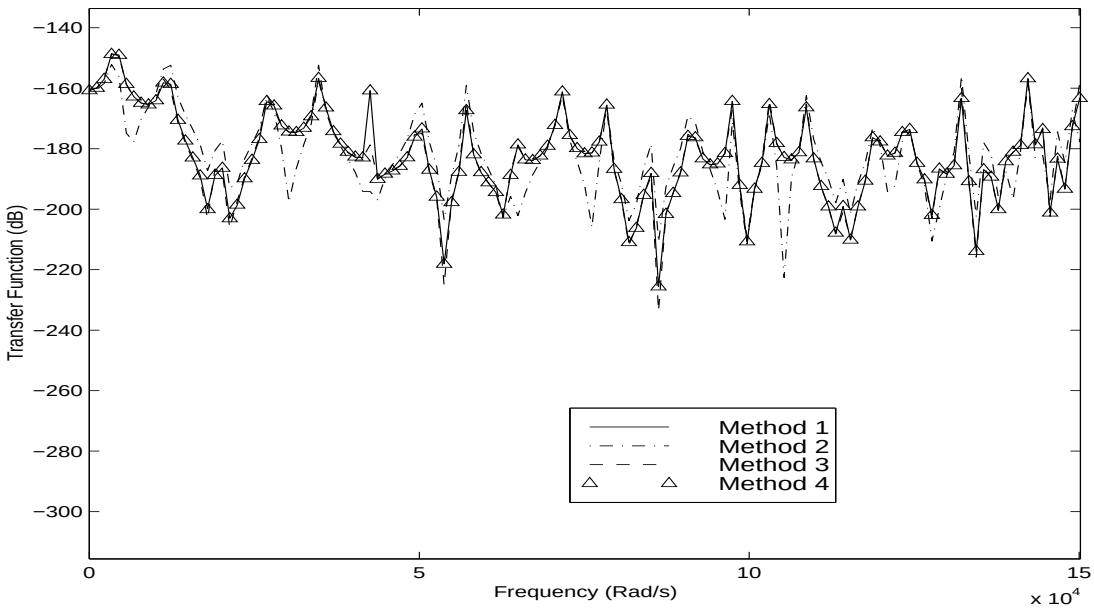

Figure 2.33: Transfer function $H_{ij}(\omega)$, $i = 11$ and $j = 24$, damping model 3, parameter set 1

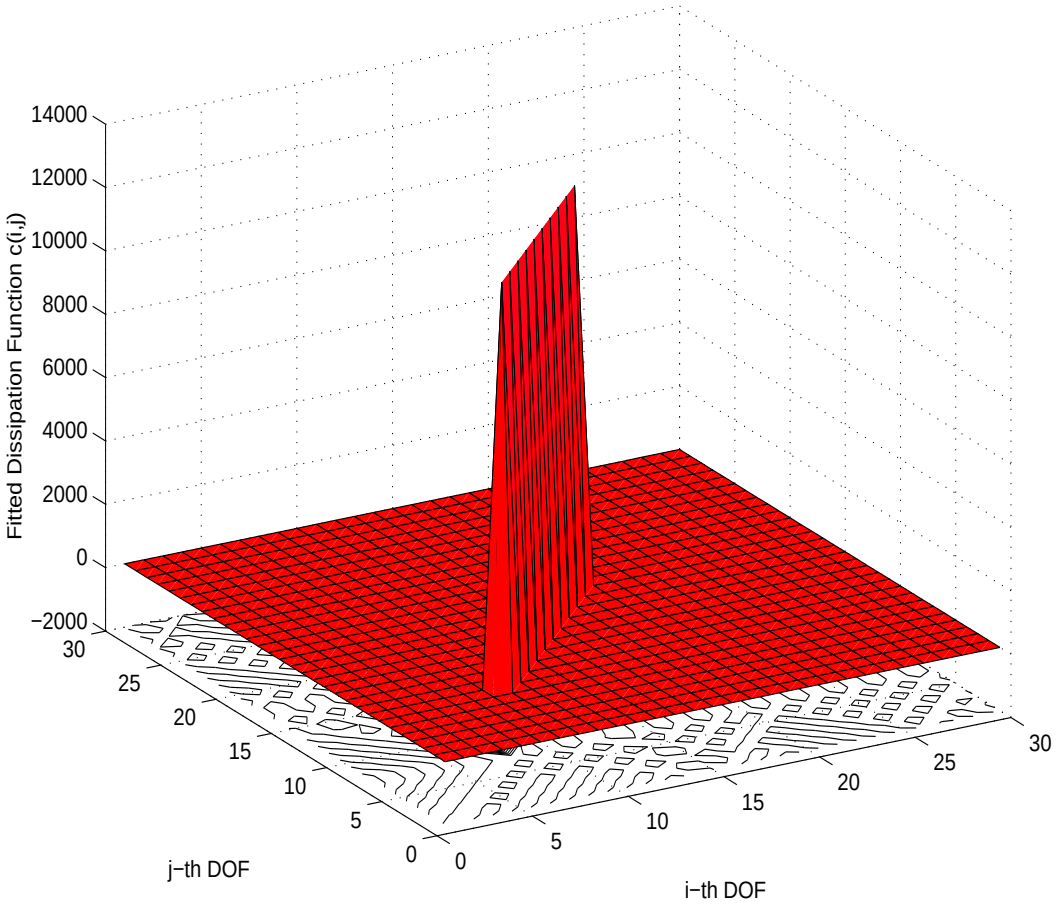

Figure 2.34: Fitted dissipation matrix c_{ij}, damping model 2, parameter set 2

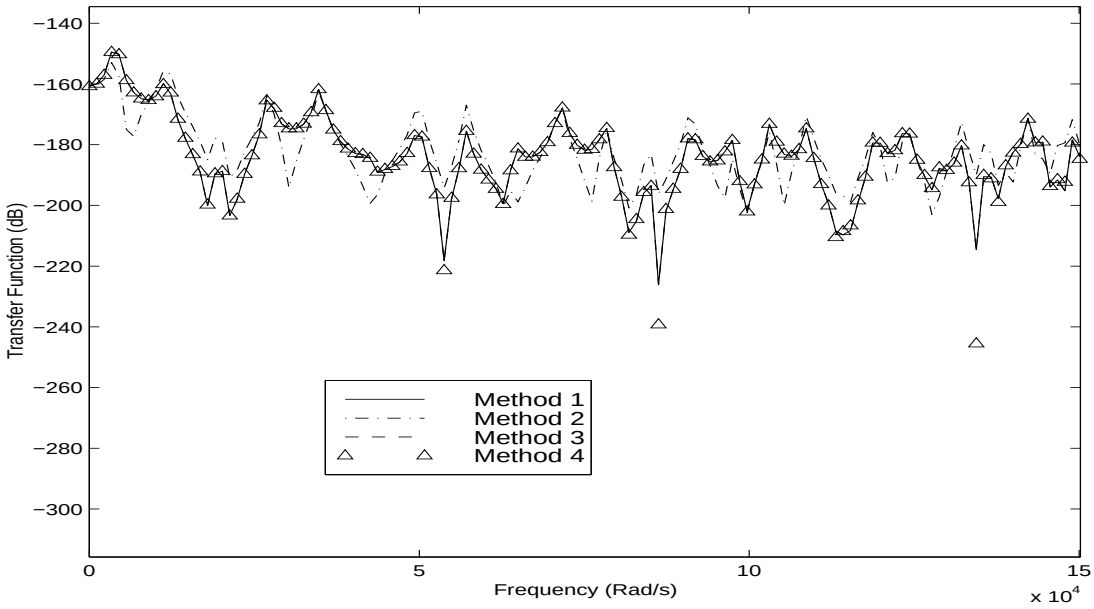

Figure 2.35: Transfer function $H_{ij}(\omega)$, $i = 11$ and $j = 24$, damping model 2, parameter set 2

Chapter 3

RESEARCH PROPOSAL

3.1 Introduction

By now it is clear that the main aim of this research project is to characterise damping in linear vibrating engineering structures. In particular this project seeks answers to a few relevant questions in this context, for example: is viscous damping a good model for damping; what can be the other possible mathematically tractable damping models; how best can we do modal analysis for a non-proportionally damped systems; is it possible to find out these models form simple measurements; can we deduce the location of damping in a general engineering structure; or, does the physics behind the damping mechanism or location of the damping at all matter from an engineering point of view; and finally, how can this uncertainty in damping be tackled for engineering predictions. In the last chapter the conventional modal analysis method for linear continuous system is extended to handle general locally reacting damping models. In conjunction with this we also have proposed a method to detect the spatial distribution of damping in vibrating structures. Doing so we have answered few of the above listed open questions, and needless to say, lots of questions remains unanswered. In this chapter we give a *research proposal* for the future of this ongoing project.

3.2 Analytical Developments of The Present Studies

Throughout the last chapter, in all our analytical treatments on continuous systems, we have considered the 'locally reacting damping' model. However, in reality, many damping models are not locally reacting. For example (see Banks and Inman, 1991) in the transverse vibration of composite beams, damping may occur due to internal friction caused from differential rates of rotation of the neighbouring beam sections. This demands relaxation of the locally-reacting damping assumption that has been made use in our previous study.

The axially vibrating rod problem we have considered in the last chapter is probably an elementary example of a continuous system. Numerical results, and thus the related physical insight, gained based on this example will not necessarily be true for other systems. It

may also be noted that from an experimental verification point of view, an axially vibrating rod example is not very suitable since it is not easy to measure the axial displacement while doing vibration testing. So for a one-dimensional structure, the methods developed are to be applied to a flexurally vibrating beam. It will also help us for a possible experimental verification of these methods since vibration testing for beams is more easy to conduct.

It is also proposed to extend our analysis to two dimensional structures. For this a rectangular plate will be considered. A small patch of damping will be introduced at different locations and the methods we have already developed will be used to detect the spatial location of this damping patches. As we know for the two dimensional structures, like plates with various boundary conditions, computational issues posses a serious problem. The finite element method (FEM) in conjunction with the procedures we have developed in the last chapter will be explored for this purpose. Other numerical procedures may also be explored.

3.3 Experimental/Numerical Studies

The purpose of the experiments to be carried out is to verify the proposed method of detection of spatial distribution of the damping. A beam will be taken and a layer (if possible movable) of damping material will be attached to some specific locations at a time. Our aim will be to detect the location of the damping layer which is already known to us. The procedure to be followed for doing this will be to find the complex modes first, and then use the method described in section 2.4.3. Location of the damping layer will also be varied for this purpose. Doing so, some particular cases of interest will be raised: for example, by placing the damping material at the ends of the beam we can simulate boundary damping.

Another series of experiments will be done on plates. A set of plates with similar material properties will be made and different damping models will be placed at different locations. The damped natural frequencies and mode shapes will be obtained by conducting usual vibration testing procedures on these structures. Following the similar method as described before we will try to obtain the spatial distribution of the damping from the complex modes. It may be noted that a combined FE study may be needed for this purpose.

The kind of experimental studies that has been proposed so far will throw light on some more theoretical questions. For example, it is well known fact that by doing an experimental modal testing it is not possible to obtain all the modes. However, the theory we have developed so far assumes that information for *all* modes is known. Moreover, the theory we have developed also assumes that all the modal data are noise free, and in that the sensitivity of the result in presence of the noise has not been considered. So a theoretical study on these issues has also been proposed.

3.4 Uncertainty In Damping

From the discussions so far, and even otherwise in accordance with general engineering wisdom, it is obvious that the measured damping parameters for a structure can not be described in a deterministic way. Say, for example, by conducting experiments on the set of similar plates as mentioned earlier, it is very much possible that we will obtain different damping parameters for different samples of plates. The probably of getting similar or different damping parameters from this experiment will of course depend on the variation of the material properties in different sample plates, care taken for conducting the experiment, environmental conditions, such as temperature, humidity and many other things. Since the causes are widely varying and difficult to detect, a realistic way to model the damping for further analysis (for example transient dynamic analysis) would be to consider it as a random quantity. Currently there has been increasing interest among the practitioners in structural dynamics to take care of this inherent randomness of the material properties. This kind of study will give a new dimension to the proposed research project. This study will not only give rise to new mathematical challenges, such as characterisation the statistics of the random complex modes, but will also throw lights in to more fundamental questions like sensitivity of the complex modes with respect to damping parameters which seems to have drawn very little attention before.

3.5 Conclusions

In this chapter we have sketched a consistent *research proposal* to be carried out by the author in the coming two years. It is hoped that a successful completion of this research project will lead towards a better understanding on the models of damping and its effect on the vibration response of engineering structures.

References

[1] Ahmadian M and Inman D J, (1984a), Classical normal modes in asymmetric nonconservative dynamic system, AIAA J., 22, 1012-1015.

[2] Ahmadian M and Inman D J, (1984b), On the nature of eigenvalues of general nonconservative systems., J. App. Mech, ASME, 51, 193-194.

[3] Baburaj V and Matsukai Y, (1994), A study on the material damping of thin angle-ply laminated plates, J. Sound. Vib., 172(3), 415-419.

[4] Bandstra J P, (1983), Comparison of equivalent viscous damping in discrete and continuous vibrating system, J. Vib. Acou. Str. and Rel. in Des., 105, 382-392.

[5] Balmès, (1997), New results on the identification of normal modes from experimental complex modes, Mech. Sys. Sgnl. Pros., 11(2), 229-243.

[6] Banks H T and Inman D J (1991), On damping mechanisms in beam, J. App. Mech, ASME., 58, 716-723.

[7] Bathe K, (1982), *Finite Element Procedures in Engineering Analysis*, Prentice-Hall Inc, New Jersey.

[8] Beards C F and Williams J L, (1977), The damping of structural vibration by rotational slip in structural joint, J. Sound. Vib., 53(3), 333-340.

[9] Bellos J and Inman D J, (1990), Frequency response of non-proportionally damped, lumped parameter, linear systems, J. Viv. Accoust., ASME, 112, 194-201.

[10] Bert C W, (1973), Material Damping: An introductory review of mathematical models, Measure and Experimental Techniques, J. Sound. Vib., 29(2), 129-153.

[11] Bhaskar A, (1995), Estimates of errors in the frequency response of non-classically damped system, J. Sound Vib, 184(1), 59-72.

[12] Bishop R E D and Price W G, (1979), An investigation into the linear theory of ship response to waves, J. Sound Vib, 62(3), 353-363.

[13] Caughey T K, (1960), Classical normal modes in damped linear dynamic system, J. App. Mech, ASME, 27, 269-271.

[14] Caughey T K and O'Kelly M E J, (1965), Classical normal modes in damped linear dynamic system, J. App. Mech, ASME, 32, 583-588.

[15] Caughey T K and Ma F, (1993), Complex modes and solvability of non-classical linear systems, J. App. Mech, ASME, 60, 26-28.

[16] Chassiakos A G, Masri S F, Smyth A W and Caughey T K, (1998), On-line identification of hysteretic systems, J. App. Mech, ASME, 65, 194-203.

[17] Chung K R and Lee C W, (1986), Dynamic reanalysis of weakly non-proportionally damped systems, J. Sound Vib, 111, 37-50.

[18] Clough R W and Mojtahedi S, (1976), Earthquake response analysis considering non-proportional damping, Earthquake. Eng. Struct. Dyn, 4, 489-496.

[19] Crandall S H, (1970), The role of damping in vibration theory, J. Sound Vib, 11(1), 3-18

[20] Crandall S H, (1991), The hysteretic damping model in vibration theory, J. Mech Eng. Sc., 205, 23-28.

[21] Cronin D L, (1976), Approximation for determining harmonically excited response of non-classically damped system, J. Eng. for Industry, ASME, 98, 43-47.

[22] Cronin D L, (1990), Eigenvalue and eigenvector determination of non-classically damped dynamic systems, Comp. and Str., 36(1), 133-138.

[23] Duncan P E and Taylor R E, (1979), A note on the dynamic analysis of non-proportionally damped systems, Earthquake. Eng. Struct. Dyn, 7, 99-105.

[24] Earls S W E, (1966), Theoretical estimation of frictional energy dissipation in a simple lap joint, J. Mech. Eng. Sci., 8(2), 207-214.

[25] Ewins D J, (1984), *Modal Testing: Theory and Practice*, Taunton: Research Studies Press.

[26] Fang J and Lyons G J, (1994), Material damping of free hanging pipes: Theoretical and experimental studies, J. Sound Vib, 172(3), 371-389.

[27] Fawzy I, (1977), Orthogonality of generally normalise eigenvector and eigenrows, AIAA J., 15(2), 276-278.

[28] Fawzy I and Bishop R E D , (1976), On the dynamics of linear non-conservative systems, Proc. Royl. soc., London, Ser- A, 352, 25-40.

[29] Felszeghy S F, (1993), On uncoupling and solving the equations of motion of vibrating linear discrete systems, J. App. Mech, ASME, 60, 456-462.

[30] Felszeghy S F, (1994), development of biorthonormal eigenvectors for modal analysis of linear discrete non-classically damped systems, 176(2), 225-269.

[31] Garvey S D and Penny J E T and Friswell M I, (1998), The relationship between the real and imaginary parts of complex modes, J. Sound Vib, 212(1), 75-83.

[32] Gawronski W and Sawicki J T, (1997), Response errors of non-proportionally lightly damped structures, J. Sound Vib, 200(4), 543-550.

[33] Hasselsman T K, (1976), Modal coupling in lightly damped structures, AIAA J., 14, 1627-1628.

[34] Hwang J H and Ma F, (1993), On the approximate solution of non-classically damped linear systems, J. App. Mech, ASME, 60, 695-701.

[35] Imregun M and Ewins D J, (1995), *Proce, 13th IMAC, Nashville, TN*, Complex modes - Origin and limits, 496-506.

[36] Inman D J, (1983), Dynamics of asymmetric non-conservative system, J. App. Mech, ASME, 50, 199-203.

[37] Lallement G and Inman D J, (1995), A tutorial on complex eigenvalues, *Proc. IMAC, Nashville, TN*, 490-495.

[38] Lazan B J, (1959), Energy dissipation mechanisms in structures with particular reference to material damping, in *Structural Dynamics*, ed Ruzcka J E, ASME annual meeting, Atlantic City, N. J.

[39] Lazan B J, (1968), *Damping of Materials and Members in Structural Mechanics*, Oxford: Pergamon Press.

[40] Liu Q K and Sneckenberger J E, (1994), Free vibration analysis of linear vibrating deficient systems with arbitrary damping, J. Sound Vib, 177(1), 43-55.

[41] Liang Z, Tong M and Lee C G, (1992), Complex modes in damped linear systems, IMAC, 791), 1-20.

[42] Malone D P, Cronin D L and Randolph T W, (1997), Eigenvalue and eigenvector determination for damped gyroscopic system, J. App. Mech, ASME, 64, 710-712.

[43] Mitchell (1990), Complex modes: a review, *Proc 8th IMAC, Kissimmee, Florida*,

[44] Ma F and Caughey T K, (1995), Analysis of linear conservative vibration, J. App. Mech, ASME, 62, 685-691.

[45] Meirovitch L, (1967), *Analytical Methods in Vibrations*, Macmillan.

[46] Meirovitch L, (1980), *Computational Methods in Structural Dynamics*, Sijthoff & Noordohoff.

[47] Nair S S and Sing R, (1986), Examination of the validity of proportional damping approximations with two further numerical indices, J. Sound Vib, 104, 348-350.

[48] Nashif A D, Jones D I G and Henderson J P, (1985), *Vibration damping*, John Wiley.

[49] Newland D E, (1989), *Mechanical Vibration Analysis and Computation*, Longman, Harlow and John Wiley, New York.

[50] Newland D E, (1987), On the modal analysis of nonconservative linear systems, J. Sound Vib, 112(1), 69-96.

[51] Nicholson D W, (1987a) Stable response of non-classically damped mechanical systems, Appl Mech Rev, ASME,

[52] Nicholson D W, (1987b), Response bounds for non-classically damped mechanical systems under transient loads, J. App. Mech, ASME, 54, 430-433.

[53] Nicholson D W and Baojiu L, (1996), Stable response of non-classically damped mechanical systems, Appl Mech Rev, ASME, 49(10)-Part 2, S49-S54.

[54] Oliveto G and Santini A, (1996), Complex modal analysis of a continuous model with radiation damping, J. Sound Vib, 192(1), 15-33.

[55] Park I W, Kim J S and Ma F, (1994), Characteristics of modal coupling in non-classically damped systems under harmonic excitation, J. App. Mech, ASME, 61, 77-83.

[56] Parter G and Sing R, Quantification of the extent on non-proportional damping discrete vibratory systems, J. Sound Vib, 104(1), 109-125.

[57] Placidi F, Poggi F and Sestieri A, (1991), Real modes computation from identified modal parameters with estimate of general damping, *Proc. 8th IMAC, London.* (1994), J. App. Mech, ASME,

[58] Paz M, (1985), *Structural Dynamics,* CBS Publishers, New Delhi.

[59] Rayleigh Lord, (1897), *Theory of Sound* (two volumes). New York: Dover Publications, second edition, 1945 re-issue.

[60] Scanlan R H, (1970), Linear damping models and causality in vibrations, J. Sound Vib, 13(4), 499-503.

[61] Sestieri A and Ibrahim S R, (1994), Analysis of errors and approximations in the use of modal coordinates, J. Sound Vib, 177(2), 145-157.

[62] Shahruz S M and Ma F, (1988), Approximate decoupling of the equations of motion of linear underdamped system, J. App. Mech, ASME, 55, 716-720.

[63] Shahruz S M, (1990), Approximate decoupling of the equations of motion of damped linear systems, J. Sound Vib, 136(1), 51-64.

[64] Shahruz S M, (1995), Comments on 'An index of damping non-proportionality for discrete vibrating systems' , *Letters to the editor*, J. Sound Vib, 186(3), 535-542.

[65] Shahruz S M and Srimatsya P A, (1997), Approximate solutions of non-classically damped linear systems in normalised and physical coordinates, J. Sound Vib, 201(2), 262-271.

[66] Tan G B, (1997), *Non-Linear Vibration of Cable-Deployed Space Structures*, Phd Thesis, Cambridge Univ. Eng. Dept.

[67] Thomson W T, Calkins C and Caravani P, (1974), A numerical study of damping, Earthquake. Eng. Struct. Dyn., 3, 97-103.

[68] Tong M, Liang Z and Lee G C, (1994), An index of damping non-proportionality for discrete vibrating systems, J. Sound Vib, 174, 37-55.

[69] Udwadia F E and Esfandiari R S, (1990), Non-classically damped dynamic systems: An iterative approach, J. App. Mech, ASME, 57, 423-433.

[70] Veletsos A S and Ventura C E, (1986), Modal analysis of non-classically damped linear systems, Earthquake. Eng. Struct. Dyn., 14, 217-243.

[71] Washed I F A and Bishop R E D, (1976), On the equation governing free and forced vibration of a general non-conservative system, J. Mech Engg Sc., 18(1), 6-10.

[72] Warburton G B and Soni S R, (1977), Errors in response calculations for non-classically damped structures, Earthu. Eng. Str. Dyn., 5, 365-376.

[73] Woodhouse J, (1998), Linear damping models for structural vibration, Submitted to J. Sound Vib.

[74] Yae K H and Inman D J, (1987), Response bounds for linear underdamped systems, J. App. Mech, ASME, 54, 419-423.

[75] Zienkiewicz O C and Morgan K, (1982), *The Finite Elements and Approximation*, John Wiley and Sons, New York.